Electronic Supplementary Material (ESI) for Polymer Chemistry.

Supporting Information

Electrostatic loading and photoredox-based release of molecular cargo from oligoviologen-crosslinked microparticles

Mark S. Palmquist, Max C. Gruschka, Jovelt M. Dorsainvil, Abigail O. Delawder, Tiana M. Saak, Mary K. Danielson, Jonathan C. Barnes*

Department of Chemistry, Washington University, St. Louis, MO 63130, USA

*E-mail: jcbarnes@wustl.edu

Table of Contents

Section A. Materials / General Methods / Instrumentation

All reagents were purchased from commercial suppliers and used without further purification unless stated otherwise. Schnucks brand 100% pure vegetable oil was purchased from Schnuck Markets, Inc. and used for laboratory use only. Grindsted polyglycerol polyricinoleate (PGPR) 90 was generously provided by Dupont Danisco as a free sample. Column chromatography was carried with silica gel (Sorbtech, 0.040 – 0.063 mm) or neutral alumina (Sorbtech, Act. 1, 0.050 – 0.2 mm). The photochemical reduction of oligoviologen-crosslinked microparticles was performed under an inert atmosphere of UHP nitrogen**.** All nuclear magnetic resonance (NMR) spectra were recorded on Varian Inova-500 with working frequencies of 500 (^{1}H) and 125 (^{13}C) MHz. Chemical shifts are reported in ppm relative to the signals corresponding to the residual non-deuterated solvent: $(CD_3)_2SO$: δ_H = 2.50 ppm; δ_C = 39.52 ppm, $CDCl_3$: δ_H = 7.26 ppm; δ_C = 77.16 ppm, and CD_2Cl_2: δ_H = 5.32 ppm; δ_C = 53.84 ppm. Matrix-assisted laser desorption/ionization time-of-flight mass spectrometry (MALDI-TOF-MS) was recorded on a Bruker Solaris 12T FT-MS and samples were prepared using 2,5-dihydroxybenzoic or α-Cyano-4-hydroxycinnamic acid matrices. Ultraviolet-Visible-Near Infrared (UV-Vis-NIR) absorbance spectra were recorded on an Agilent Cary 5000 spectrophotometer with a PbSmart NIR detector. Photochemical reduction of the oligoviologen-based microparticles soaked in triethanolamine was accomplished using two Hampton Bay desk lamps with ABI LED aquarium light bulbs (450 nm / 12 Watt / 740 lumens). To aid in the precipitation of viologen-based compounds from their crude reaction mixtures, a Thermo Scientific Sorvall ST 8 small benchtop centrifuge was employed. Optical microscopy images were taken using a Thermo Fisher Scientific EVOS XL Core microscope with the 40X objective, 20/40 phase contrast filter, and a 3.1 megapixel camera. Dynamic light scattering (DLS) data was recorded on Malvern ZEN3600 equipment. Scanning electron microscopy (SEM) was conducted using a Thermofisher Quattro S ESEM apparatus with a high-stability Schottky field emission gun electron source providing electron resolution of 0.7 nm at 30 keV, 1.4 nm at 1 keV. Dialysis membrane tubing was purchased from Spectrum Labs. Spectra/Por 7 regenerated cellulose tubing with an 8 kD molecular weight cut-off was used for all release kinetics experiments. Spectrum brand plastic clips were used to secure each end of the tubing.

Section B. Synthetic Protocols

1) Synthesis of Hexaethylene glycol di-p-toluenesulfonate (1)

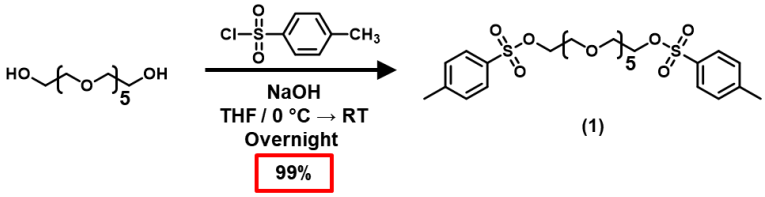

Hexaethylene glycol (5.0 g, 4.44 mL, 17.7 mmol, 1 equiv) was dissolved in THF (25 mL) and cooled to 0 °C. NaOH (4.25 g, 106.3 mmol, 6 equiv) was dissolved in deionized water (5 mL) and added slowly. The reaction was stirred at 0 °C for 30 min. *p*-toluenesulfonyl chloride (13.5 g, 70.8 mmol, 4 equiv) was dissolved in THF (25 mL) and added to the flask by slow-addition funnel over the course of 30 min. The reaction was kept at 0 °C for 1 h before warming to RT and stirring 18 h. The reaction mixture was concentrated by rotary evaporation and then dissolved into CH_2Cl_2 (100 mL) followed by washing with brine solution (40 mL). The organic layer was collected, dried with Na_2SO_4, and concentrated by rotary evaporation. The crude product was purified by silica column chromatography: loaded in CH_2Cl_2 and eluted in 3% MeOH:CH_2Cl_2. TLC in 5% MeOH:CH_2Cl_2 was used to track column progress. The product fractions were collected, concentrated by rotary evaporation, and dried under vacuum to yield **(1)** as a clear, viscous oil (10.42 g, 99% yield). ^{1}H NMR 500 MHz, ($CDCl_3$): δ_H 7.79 (d, J = 8.3 Hz, 4H); 7.34 (d, J = 8.1 Hz, 4H); 4.17 – 4.13 (m, 4H); 3.69 – 3.66 (m, 4H); 3.62 – 3.60 (m, 8H); 3.57 (s, 8H); 2.44 (s, 6H). ^{13}C NMR (125 MHz, $CDCl_3$): δ_C 144.77, 129.80, 127.96, 70.74, 70.61, 70.55, 70.50, 69.23, 68.67, 21.63. MALDI-TOF for ***DiTos HEG***; Calcd for $C_{26}H_{38}O_{11}S_2$: m/z = 613.175 $[M + Na]^+$; Found: 613.373 $[M + Na]^+$.

2) Synthesis of 2V•2OTs (2)

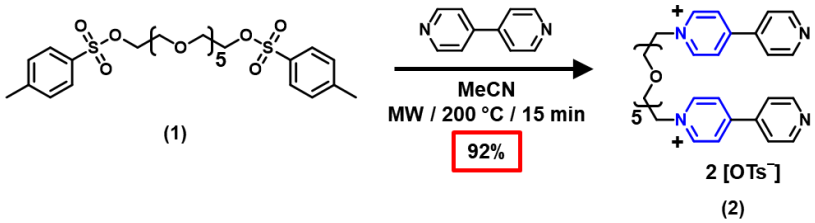

(1) (2)

(1) (500 mg, 0.86 mmol, 1 equiv) and 4,4'-bipyridine (2.64 g, 16.92 mmol, 20 equiv) were dissolved in MeCN (20 mL) in a 35 mL microwave high-pressure vial (CEM part 909036) equipped with a small stir bar. The vial was reacted in a CEM microwave at 150 W for 15 min to 200 °C and 300 psi. The resulting dark brown/black solution was transferred to four 50 mL centrifuge tubes (~5 mL per tube) and diluted to 50 mL with Et_2O. The tubes were centrifuged at 4500 rpm for 5 min. The supernatant was decanted away, the solid was re-dissolved in a minimal amount of MeOH and diluted to 50 mL with Et_2O. The previous two steps were repeated three times. The resulting brown/black, oily product was dried overnight to yield **(2)** as a brown solid (705 mg, 92% yield). ^{1}H NMR (500 MHz, $(CD_3)_2SO$): δ_H 9.16 (t, J = 7.4 Hz, 4H); 8.92 – 8.83 (m, 4H); 8.62 (t, J = 7.3 Hz, 4H); 8.10 – 8.01 (m, 4H); 7.47 (d, J = 8.0 Hz, 4H); 7.09 (d, J = 7.8 Hz, 4H); 4.85 – 4.78 (m, 4H); 3.93 (dd, J = 12.3, 7.7 Hz, 4H); 3.60 – 3.44 (m, 18H); 2.26 (s, 6H). ^{13}C NMR (125 MHz, $(CD_3)_2SO$): δ_C 152.69, 151.00, 146.27, 146.13, 141.71, 138.10, 128.53, 125.94, 125.49, 122.56, 70.11, 70.08, 69.90, 69.05, 60.38, 21.21. MALDI-TOF for ***(2)***; Calcd for $C_{39}H_{47}N_4O_8S$: m/z = 731.31 $[M - OTs]^+$; Found: 731.639 $[M - OTs]^+$.

3) Synthesis of 2V-St • 4Cl (3)

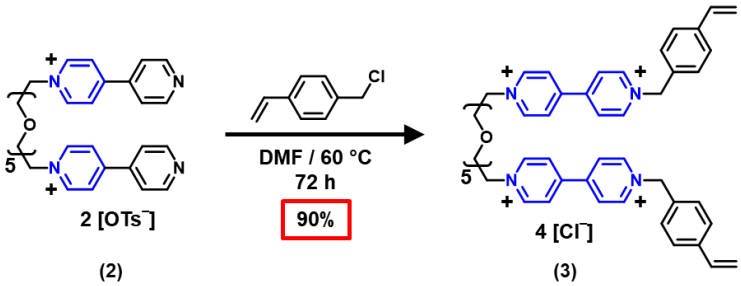

(2) (3)

(2) (1 g, 1.11 mmol, 1 equiv) and 4-vinylbenzyl chloride (6.76 g, 6.24 mL, 44.28 mmol, 40 equiv) were dissolved in DMF (dry, 20 mL, 50 mg·mL^{-1} **(2)**) and heated to 60 °C for 72 h. The reaction vessel was cooled to RT and the solution was transferred into four 50 mL centrifuge tubes and diluted to 50 mL with Et_2O. The tubes were centrifuged at 4500 rpm for 2 min. The supernatant was decanted away, the solid was re-dissolved in a minimal amount of MeOH and diluted to 50 mL with Et_2O. The previous two steps were

repeated three times. The solid was dried to yield **2V-St** • 2OTs 2Cl as a brown solid (1.20 g, 90% yield). **2V-St** • 2OTs 2Cl was converted to **2V-St** • 4 PF_6 by dissolving in H_2O followed by the addition of excess ammonium hexafluorophosphate (NH_4PF_6). The product precipitate was collected by centrifugation. The supernatant was decanted and the solid was re-washed with H_2O by centrifugation three times before drying under vacuum. The solid was then converted to **(3)** by dissolving in minimal MeCN followed by the addition of excess tetrabutylammonium chloride (TBACl). The product precipitate was collected by centrifugation. The supernatant was decanted and the solid was re-washed with MeCN by centrifugation three times before drying under vacuum yielding **(3)** as a brown solid (913 mg, 88% yield). ^{1}H NMR (500 MHz, $(CD_3)_2SO$): δ_H 9.66 (d, *J* = 6.6 Hz, 4H); 9.41 (d, *J* = 6.6 Hz, 4H); 8.87 (d, *J* = 6.6 Hz, 4H); 8.84 (d, *J* = 6.6 Hz, 4H); 7.66 (d, *J* = 8.1 Hz, 4H); 7.56 (d, *J* = 8.1 Hz, 4H); 6.74 (dd, *J* = 17.6, 11.0 Hz, 2H); 6.01 (s, 4H); 5.89 (d, *J* = 17.7 Hz, 2H); 5.32 (d, *J* = 10.9 Hz, 2H); 4.96 – 4.90 (m, 4H); 4.00 – 3.94 (m, 4H); 3.57 – 3.53 (m, 4H); 3.49 – 3.36 (m, 12H). ^{13}C NMR (125 MHz, $(CD_3)_2SO$): δ_C 149.20, 146.70, 146.24, 138.66, 136.26, 134.23, 129.95, 127.61, 127.28, 126.82, 116.23, 70.11, 70.04, 69.92, 69.11, 63.11, 60.61.

4) Synthesis of [Ru(BpyMe$_2$)]Cl$_2$ (4)

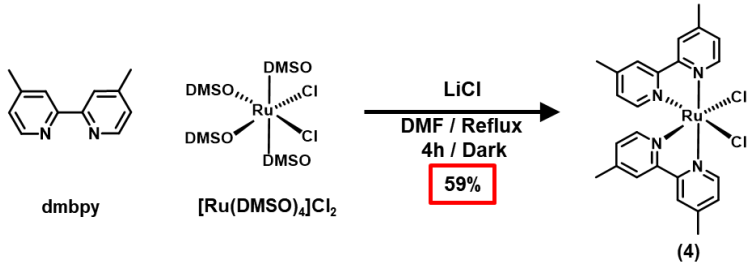

(4) was synthesized by modifying a previously reported synthesis.[1] Briefly, $[Ru(DMSO)_4]Cl_2$ (2.00 g, 4.13 mmol, 1 equiv), 4,4′-dimethyl-2,2′-bipyridine (dmbpy) (1.52 g, 8.26 mmol, 2 equiv), and LiCl (8.75 g, 206.4 mmol, 50 equiv) were dissolved in DMF (50 mL) and heated to reflux while covered in aluminium foil for 4 h. The product was allowed to cool slightly before pouring into a flask containing Me_2CO (800 mL). The flask was placed in a freezer overnight. The solid precipitate that resulted was filtered and washed with H_2O to remove salts and $Ru(bpy)_3$ by-product until the filtrate was clear and colourless. The product was dried to yield **(4)** as black powder (1.16 g, 52% yield). ^{1}H NMR (500 MHz, CD_2Cl_2): δ_H 9.91 (d, *J* = 5.5 Hz, 2H); 7.99 (s, 2H); 7.87 (s, 2H); 7.40 (t, *J* = 5.5 Hz, 4H); 6.76 (d, *J* = 4.7 Hz, 2H); 2.62 (s, 6H); 2.44 (s, 6H). MALDI-TOF for **(4)**; Calcd for $C_{24}H_{24}Cl_2N_4Ru$: *m/z* = 505.073 [*M* - Cl]$^+$; Found: 505.228 [*M* - Cl]$^+$.

5) Synthesis of THP-Protected 6-Chlorohexan-1-ol (5)

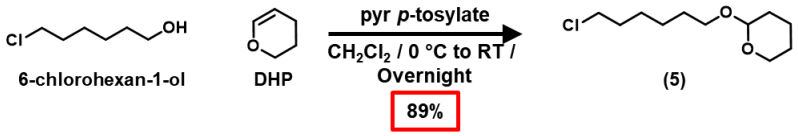

(5) was synthesized by modifying a previously reported synthesis.[2] Briefly, 6-chlorohexan-1-ol (6.83 g, 6.67 mL, 50 mmol, 1 equiv) and pyridinium *p*-toluene sulfonate (pyr *p*-tosylate) (1.26 g, 10 mmol, 0.2 equiv) were added with dry CH_2Cl_2 (100 mL) to an oven-dried flask at 0 °C under N_2. 3,4-dihyro-2H-pyran (DHP) (8.41 g, 9.12 mL, 100 mmol, 2 equiv) was added dropwise by syringe and the solution was stirred for 30 min at 0 °C. The solution was allowed to warm to RT while stirring overnight. The solution was washed in a separatory funnel with saturated $NaHCO_3$ (2 x 30 mL) and brine (1 x 30 mL). The organic layers were collected, dried with Na_2SO_4, and concentrated by rotary evaporation. Product was purified by silica column chromatography: crude mixture was loaded in hexanes and ramped up to 3:97 EtOAc:Hexanes. The product fractions were collected and concentrated by rotary evaporation. The product was dried to yield **(5)** as a light yellow, clear oil (9.79 g, 89% yield). ^{1}H NMR (500 MHz, CD_2Cl_2): δ_H 4.53 (t, J = 3.8 Hz, 1H); 3.82 (m, 1H), 3.69 (dt, J = 9.6, 6.7 Hz, 1H), 3.55 (t, J = 6.8 Hz, 2H), 3.45 (m, 1H), 3.35 (dt, J = 9.6, 6.5 Hz, 1H), 1.79 (m, 3H), 1.67 (m, 1H), 1.45 (m, 11H). ^{13}C NMR (125 MHz, CD_2Cl_2): δ_C 98.74, 67.18, 62.06, 45.21, 32.61, 30.79, 29.59, 26.70, 25.57, 19.66. MALDI-TOF for **(5)**; Calcd for $C_{11}H_{21}ClO_2$: *m/z* = 243.113 [M + Na]$^+$; Found: 243.317 [M + Na]$^+$.

6) Synthesis of Protected Heptyl Bpy (6)

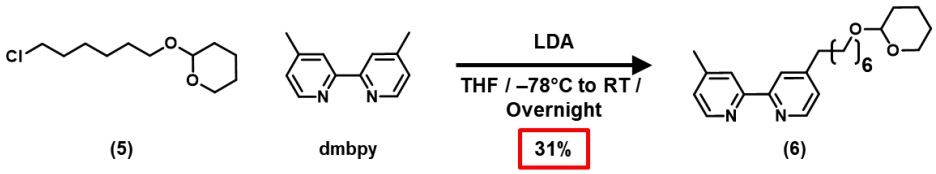

(6) was synthesized by modifying a previously reported synthesis.[3] Briefly, dmbpy (0.50 g, 2.71 mmol, 1 equiv) was added to an oven-dried round bottom flask and dissolved in dry THF (15 mL). The solution was cooled to –78 °C and under N_2. In a separate flask, distilled diisopropylamine (0.25 g, 0.34 mL, 2.44 mmol, 0.9 equiv) was added with dry THF (5 mL) and cooled to –78 °C. *n*-Butyl lithium (0.97 mL, 2.5 M solution in hexane, 2.44 mmol, 0.9 equiv) was added by syringe and the solution was stirred for 30 min to yield lithium diisopropylamide (LDA). The LDA solution was then transferred by syringe and added dropwise to the flask containing dimethyl bipyridine. The solution turned darker brown/black with each drop upon addition. The solution was stirred for 2 h. **(5)** (0.90 g, 4.07 mmol, 1.5 equiv) was added as a solution in dry THF (5 mL)

by syringe. The solution was stirred for 30 min at –78 °C before warming to RT and stirring overnight. The reaction was quenched with H_2O (5 mL). The product solution was combined with brine (50 mL) and extracted into Et_2O (2 washes of 50 mL). The organic layer was collected, dried by Na_2SO_4, and concentrated by rotary evaporation. The crude product was recovered as a yellow oil and purified by silica column chromatography: loaded and eluted in 50:50 EtOAc:CH_2Cl_2 eluent. The TLC plates used to track column progress were eluted in 10% MeOH in CH_2Cl_2 to identify product. The product fractions were collected and concentrated by rotary evaporation. The desired product, **(6)**, was isolated as a light-yellow oil (0.31 g, 31% yield). ^{1}H NMR (500 MHz, CD_2Cl_2): δ_H 8.51 (dd, *J* = 7.4, 5.0 Hz, 2H); 8.28 (s, 2H); 7.15 (d, *J* = 3.1 Hz, 2H); 4.53 (t, *J* = 3.8 Hz, 1H); 3.81 (ddd, *J* = 11.3, 8.2, 3.4 Hz, 1H); 3.68 (dt, *J* = 9.6, 6.8 Hz, 1H); 3.47 – 3.42 (m, 1H); 3.34 (dt, *J* = 9.6, 6.6 Hz, 1H); 2.73 – 2.68 (m, 2H); 2.44 (s, 3H); 1.83 – 1.74 (m, 1H); 1.73 – 1.61 (m, 3H); 1.59 – 1.44 (m, 6H); 1.40 – 1.33 (m, 6H). ^{13}C NMR (125 MHz, CD_2Cl_2): δ_C 148.64, 144.52, 124.61, 123.93, 121.83, 98.72, 67.35, 62.05, 35.42, 30.80, 30.39, 29.72, 29.23, 29.19, 26.13, 25.58, 20.95, 19.68. MALDI-TOF for **(6)**; Calcd for $C_{23}H_{32}N_2O_2$: *m/z* = 391.236 [*M* + Na]$^+$; Found: 391.313 [*M* + Na]$^+$.

7) Synthesis of Hydroxyheptyl Bpy (7)

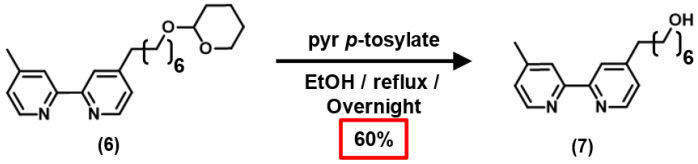

(7) was synthesized by modifying a previously reported synthesis.[3] Briefly, **(6)** (0.20 g, 0.54 mmol, 1 equiv) and pyr *p*-tosylate (0.14 g, 0.54 mmol, 1 equiv) were added to a round bottom flask and dissolved in EtOH (20 mL). The solution was heated to reflux overnight. The product solution was concentrated by rotary evaporation and redissolved in CH_2Cl_2 (50 mL). The product solution was washed with saturated $NaHCO_3$ (2 x 30 mL) and with brine (30 mL). The organic layer was collected, dried by Na_2SO_4, and concentrated by rotary evaporation. The crude product was recovered as a yellowish oil and purified by silica column chromatography: loaded in 10:90 EtOAc:CH_2Cl_2 and ramped up to 20:80 EtOAc:CH_2Cl_2 eluent until excess pyridinium impurity was eluted. The eluent polarity was increased to pure EtOAc to elute product. The TLC plates were eluted in 10% MeOH in CH_2Cl_2 to identify product. The product fractions were collected and concentrated by rotary evaporation. The desired product, **(7)**, was isolated as a white solid (0.08 g, 60%

yield). ^{1}H NMR (500 MHz, CD_2Cl_2): δ_H 8.54 (dd, *J* = 8.1, 5.0 Hz, 1H); 8.32 (s, 1H); 7.19 (d, *J* = 4.9 Hz, 1H); 3.61 (t, *J* = 6.6 Hz, 1H); 2.76 – 2.71 (m, 1H); 2.47 (s, 1H); 1.73 (dt, *J* = 15.0, 7.5 Hz, 1H); 1.55 (dt, *J* = 13.4, 6.6 Hz, 1H); 1.44 – 1.34 (m, 3H). ^{13}C NMR (125 MHz, CD_2Cl_2): δ_C 148.58, 148.43, 124.72, 124.08, 122.01, 121.27, 62.67, 35.39, 32.75, 30.25, 29.09, 25.57, 20.99. MALDI-TOF for **(7)**; Calcd for $C_{18}H_{24}N_2O$: *m/z* = 285.196 $[M + H]^+$; Found: 285.232 $[M + H]^+$.

8) Synthesis of Ru(Bpy)$_3$ Heptanol (8)

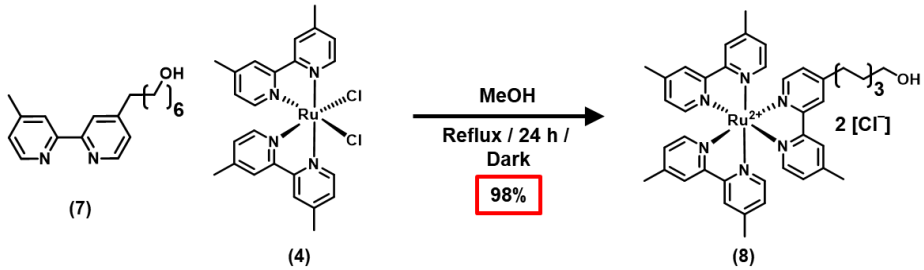

(8) was synthesized by modifying a previously reported synthesis.[4] Briefly, **(4)** (500 mg, 0.93 mmol, 1 equiv) and **(7)** (278 mg, 1.30 mmol, 1.4 equiv) were added to a round bottom flask and dissolved in MeOH (50mL). The round bottom flask was heated to reflux while covered in aluminium foil for 24 h. The deep red solution was concentrated to ~5 mL, which was then transferred to 50 mL centrifuge tubes by pipette, using MeCN (minimal) to ensure complete transfer. The product was diluted to 50 mL with Et_2O, causing a bright red-orange product to precipitate. The mix was centrifuged at 4500 rpm for 5 min. The supernatant was decanted away, and the product was washed again with Et_2O. The wash and centrifuge steps were repeated 3 times. The solid product was collected and dried to yield **(8)** as a vibrant red-orange powder (682 mg, 98% yield). ^{1}H NMR (500 MHz, CD_2Cl_2): δ_H 8.85 (s, 1H); 8.74 (d, *J* = 12.1 Hz, 5H); 7.50 (dt, *J* = 9.9, 4.8 Hz, 6H); 7.24 (dd, *J* = 15.6, 7.1 Hz, 6H); 3.52 (t, *J* = 6.4 Hz, 2H); 2.83 (dd, *J* = 13.7, 6.0 Hz, 2H); 2.60 (d, *J* = 4.9 Hz, 15H); 1.78 – 1.70 (m, 2H); 1.50 – 1.44 (m, 2H); 1.34 (d, *J* = 3.2 Hz, 6H). ^{13}C NMR (125 MHz, CD_2Cl_2): δ_C 156.81, 156.75, 156.71, 156.69, 156.67, 156.63, 154.85, 150.44, 150.33, 150.28, 150.14, 150.06, 150.00, 149.91, 128.46, 128.42, 125.69, 125.61, 125.01, 61.76, 35.04, 32.51, 29.56, 28.60, 28.55, 25.29, 21.08, 21.03. MALDI-TOF for **(8)**; Calcd for $C_{42}H_{48}Cl_2N_6ORu$: *m/z* = 754.292 $[M - 2Cl + e^-]^+$; Found: 754.650 $[M - 2Cl + e^-]^+$.

9) Synthesis of Ru(bpy)$_3$ Ac (9)

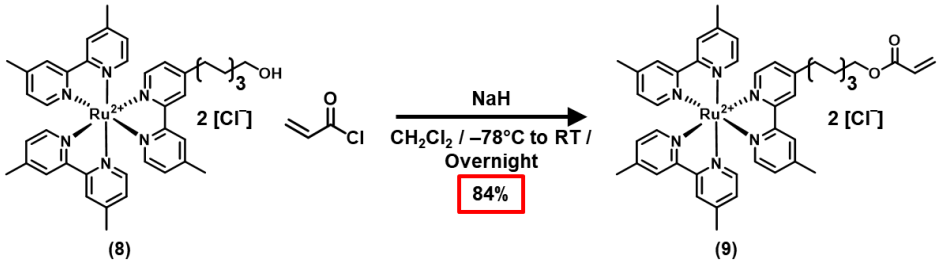

(8) (9)

(8) (50 mg, 0.060 mmol, 1 equiv) was added to an oven-dried flask with dry CH_2Cl_2 (45 mL). The flask was cooled to –78 °C and NaH (60% dispersion in mineral oil, 1.75 mg, 0.073 mmol, 1.2 equiv) was added. The flask was sealed under N_2 and stirred for 1 h. Acryloyl chloride (0.27 g, 0.25 mL, 3.03 mmol, 50 equiv) was added slowly by syringe. The round bottom flask was then warmed to RT overnight. The product was concentrated to ~5 mL which was then transferred to 50 mL centrifuge tubes by pipette. The solution was transferred to 50 mL centrifuge tubes by pipette, using MeOH (minimal) to ensure complete transfer. Product was diluted to 50 mL with Et_2O, causing a bright red-orange product to precipitate. The mix was centrifuged at 4500 rpm for 5 min. The supernatant was decanted away, and the product was washed again with Et_2O. The wash and centrifuge steps were repeated 3 times. The product was further purified by neutral alumina column chromatography: loaded in pure CH_2Cl_2 eluent and then ramped to 4% MeOH in CH_2Cl_2. Coloured fractions were collected and concentrated by rotary evaporation. Product was collected and dried to yield **(9)** as a red-orange powder (45 mg, 84% yield). ^{1}H NMR (500 MHz, CD_2Cl_2): δ_H 8.82 (d, *J* = 19.8 Hz, 4H); 8.69 (d, *J* = 39.9 Hz, 2H); 7.55 – 7.46 (m, 6H); 7.23 (dd, *J* = 12.7, 6.4 Hz, 6H); 6.34 (dd, *J* = 17.3, 1.5 Hz, 1H); 6.10 (dd, *J* = 17.3, 10.4 Hz, 1H); 5.80 (dd, *J* = 10.4, 1.5 Hz, 1H); 4.11 (t, *J* = 6.7 Hz, 2H); 2.84 (dd, *J* = 15.5, 7.5 Hz, 2H); 2.61 (s, 15H); 1.72 (dd, *J* = 14.5, 7.3 Hz, 2H); 1.68 – 1.62 (m, 2H); 1.42 – 1.34 (m, 6H). ^{13}C NMR (125 MHz, CD_2Cl_2): δ_C 156.72, 150.40, 149.95, 130.09, 128.62, 128.44, 127.56, 125.82, 125.76, 124.75, 64.43, 35.18, 29.98, 29.15, 28.91, 28.52, 25.74, 21.06. MALDI-TOF for **(9)**; Calcd for $C_{45}H_{50}Cl_2N_2O_2Ru$: *m/z* = 808.303 [*M* - 2Cl + e^-]$^+$; Found: 808.707 [*M* - 2Cl + e^-]$^+$.

10) Synthesis of Hydroxy-Tetraphenyl Porphyrin (10)

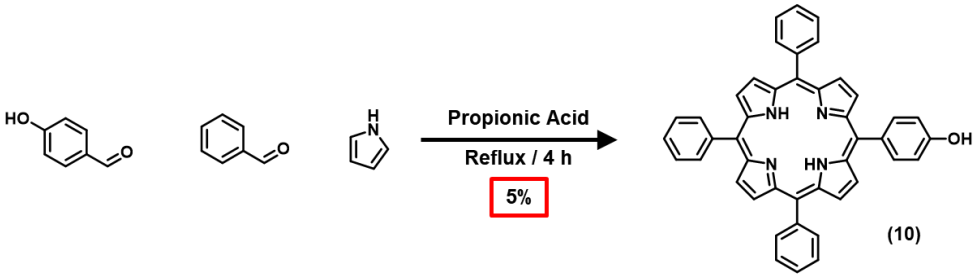

(10) was synthesized according to a previously reported literature procedure.[5] Benzaldehyde (5.7 g, 53.7 mmol, 3 equiv) and 4-hydroxybenzaldehyde (2.18 g, 17.9 mmol, 1 equiv) were dissolved in propionic acid (180 mL). This solution was heated to reflux at 140 °C for 30 min. Pyrrole (4.79 g, 71.6 mmol, 4 equiv) was added dropwise to the solution under N_2. The reaction mixture was refluxed for 4 h and then cooled to RT. Then, approximately half the volume of the reaction mixture was removed by rotary evaporation, and MeOH (250 mL) was added to the concentrated solution. The resultant dark blue solution was stored overnight at 4 ˚C. After filtration, the purple precipitate was collected and washed with cold MeOH. The crude product was dried under vacuum and subsequently purified by column chromatography using Hexane:CH_2Cl_2 (1:1 → 0:1) as the eluent to yield the desired product, **(10)**, as a purple solid (0.48 g, 5 % yield). ^{1}H NMR (500 MHz, CD_2Cl_2): δ_H 8.96 – 8.84 (m, 8H); 8.25 (d, *J* = 7.5 Hz, 6H); 8.12 – 8.08 (m, 2H); 7.85 – 7.77 (m, 9H); 7.25 – 7.20 (m, 2H); -2.80 (s, 2H).^{13}C NMR (125 MHz, $CDCl_3$): δ_C 142.19, 135.68, 134.55, 127.69, 126.67, 113.65. MALDI-TOF for ***(10)***; Calcd for $C_{44}H_{30}N_4O$: *m/z* = 630.242 $[M]^+$; Found: 630.495 $[M]^+$.

11) Synthesis of Monotosylated Poly(ethylene glycol)$_{45}$ (11)

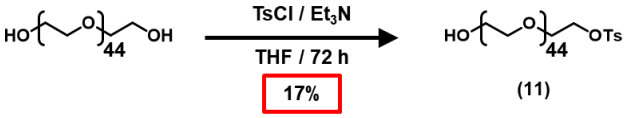

(11) was synthesized according to a modified previously reported literature procedure.[5] Polyethylene glycol (M_W 2000 Da) (10 g, 5.0 mmol, 1 equiv), *p*-TsCl (0.86 g, 4.0 mmol, 0.8 equiv) and Et_3N (1.15 mL, 8.0 mmol, 1.6 equiv) in 100 mL dry THF were stirred under N_2 for 72 h. The mixture was filtered and concentrated by rotary evaporation. The product was purified by column chromatography using CH_2Cl_2:MeOH (1:0 → 93:7) as eluent to yield the desired product, **(11)**, as a white solid (1.86 g, 17% yield). ^{1}H NMR (500 MHz, $CDCl_3$): δ_H 7.79 – 7.76 (m, 2H); 7.32 (d, *J* = 8.0 Hz, 2H); 4.14 (dd, *J* = 5.4, 4.4 Hz, 2H); 3.77 – 3.74 (m, 2H); 3.72 – 3.68 (m, 3H); 3.68 – 3.57 (m, 188H); 3.48 (dd, *J* = 5.6, 4.2 Hz, 2H); 2.72 (s, 4H); 2.43 (s, 3H). ^{13}C NMR (125 MHz, $CDCl_3$): δ_C 129.79, 127.95, 72.50, 70.55, 70.31, 69.21, 68.66, 61.70.

12) Synthesis of TPP−PEG-OH (12)

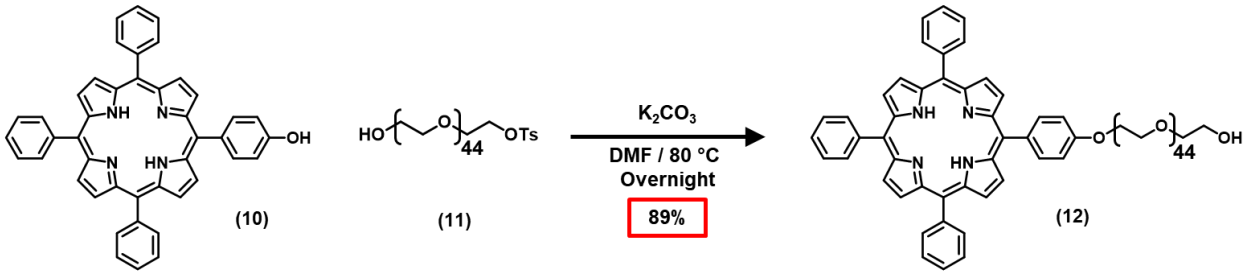

(12) was synthesized according to a modified previously reported literature procedure.[5] **(10)** (0.4 g, 0.63 mmol, 2 equiv), **(11)** (0.63 g, 0.31 mmol, 1.0 equiv), and K_2CO_3 (0.88 g, 6.32 mmol, 20 equiv) in 45 mL dry DMF were heated to 80 °C under N_2 for 12 h. The mixture was filtered and dried completely by rotary evaporation. The product was loaded on a silica column and eluted by CH_2Cl_2 to recover unreacted **(10)** before the solvent polarity was increased to elute the product **(12)** in CH_2Cl_2:MeOH 85:15. The product fractions were concentrated by rotary evaporation. The final product was dissolved in Me_2CO and CH_2Cl_2 and passed through a 0.45 µ PTFE (hydrophobic) filter to remove the silica gel that dissolved in the excess MeOH used as column eluent. The solution was concentrated by rotary evaporation and dried by lyophilization to yield **(12)** as a purple solid (0.75 g, 89% yield). ^{1}H NMR (500 MHz, CD_2Cl_2): δ_H 8.93 – 8.85 (m, 8H), 8.24 (d, *J* = 7.6 Hz, 6H), 8.16 – 8.11 (m, 2H), 7.79 (d, *J* = 6.0 Hz, 9H), 7.37 – 7.31 (m, 2H), 4.46 – 4.41 (m, 2H), 4.04 (d, *J* = 5.7 Hz, 2H), 3.82 (d, *J* = 2.3 Hz, 2H), 3.75 (d, *J* = 3.0 Hz, 2H), 3.71 – 3.67 (m, 4H), 3.67 – 3.52 (m, 150H). ^{13}C NMR (125 MHz, $CDCl_3$): δ_C 135.53, 134.53, 127.68, 126.66, 112.86, 70.56.

13) Synthesis of TPP−PEG–Ac (13)

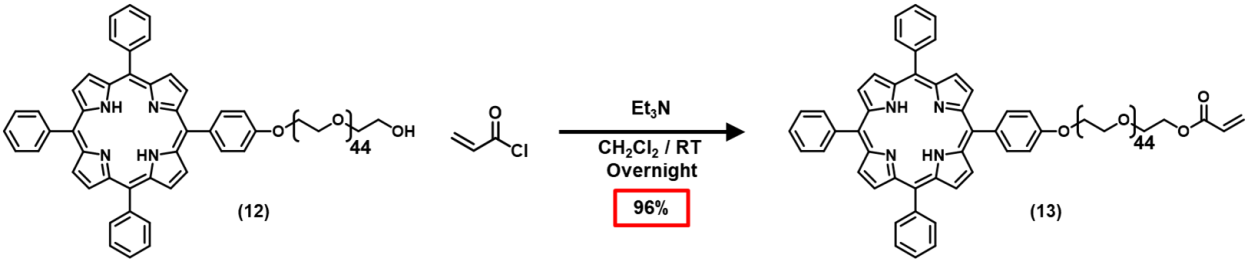

(13) was synthesized according to a modified previously reported literature procedure.[5] **(12)** (0.5 g, 0.19 mmol, 1 equiv), and Et_3N (0.08 g, 0.76 mmol, 4 equiv) were dissolved in dry CH_2Cl_2 (20 mL) under N_2. The solution was stirred at RT for 30 min and acryloyl chloride (0.05 g, 0.57 mmol, 3 equiv) in CH_2Cl_2 (5 mL) was added dropwise. The reaction mixture was stirred at RT overnight and then diluted with CH_2Cl_2 (100 mL). The product solution was washed with saturated $NaHCO_3$ (1 × 50 mL) and H_2O (1 × 50 mL). The combined organic phases were dried with Na_2SO_4, filtered, and concentrated by rotary evaporation. The

product was dried by lyophilization to yield **(13)** as a purple solid (0.49 g, 96% yield). ^{1}H NMR (500 MHz, CD_2Cl_2): δ_H 8.96 – 8.85 (m, 8H); 8.28 – 8.23 (m, 6H); 8.17 – 8.14 (m, 2H); 7.86 – 7.77 (m, 9H); 7.37 – 7.33 (m, 2H); 6.42 (dd, *J* = 17.3, 1.4 Hz, 1H); 6.21 – 6.15 (m, 1H); 5.87 (dt, *J* = 10.4, 1.5 Hz, 1H); 4.46 – 4.43 (m, 2H); 4.32 – 4.29 (m, 2H); 4.06 – 4.03 (m, 2H); 3.84 (dd, *J* = 5.7, 3.5 Hz, 2H); 3.76 (dd, *J* = 5.7, 3.6 Hz, 3H); 3.74 – 3.71 (m, 4H); 3.64 – 3.59 (m, 167H); -2.80 (s, 2H). ^{13}C NMR (125 MHz, $CDCl_3$): δ_C 134.53, 133.21, 130.97, 128.29, 127.68, 126.66, 70.57.

14) Synthesis of ZP–PC (14)

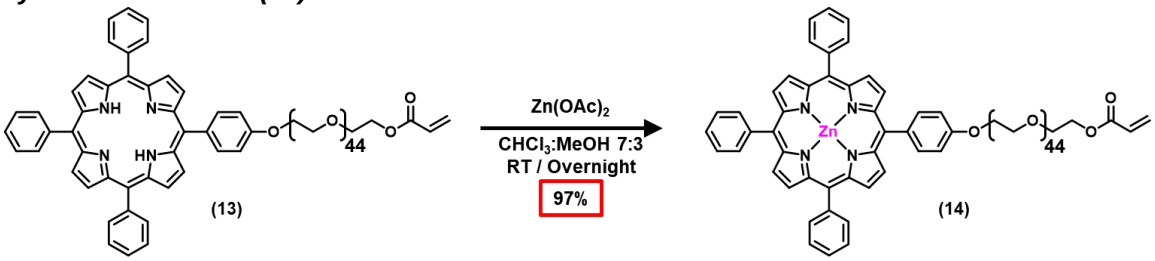

(14) was synthesized according to a modified previously reported literature procedure.[5] **(13)** (0.3 g, 0.11 mmol, 1 equiv), and $Zn(OAc)_2$ (0.24 g, 1.11 mmol, 10 equiv) were dissolved in a (70:30) $CHCl_3$: MeOH mixture (30 mL) and stirred overnight while wrapped in Al foil. The reaction mixture was diluted with $CHCl_3$ (50 mL) and washed with H_2O (50 mL). The combined organic phases were dried with Na_2SO_4, filtered, and concentrated by rotary evaporation. The final product was then dissolved in Me_2CO and CH_2Cl_2 mixture and passed through a 0.45 µ PTFE (hydrophobic) filter to remove any unreacted salt. The product was dried by lyophilization to yield product **(14)** as a vibrant purple solid (0.3 g, 97% yield). ^{1}H NMR (500 MHz, CD_2Cl_2): δ_H 8.97 (dd, *J* = 23.4, 4.4 Hz, 8H); 8.24 (d, *J* = 6.6 Hz, 6H); 8.14 (d, *J* = 8.1 Hz, 2H); 7.85 – 7.73 (m, 9H); 7.34 (dd, *J* = 8.3, 4.7 Hz, 2H); 6.43 – 6.37 (m, 1H); 6.20 – 6.13 (m, 1H); 5.87 – 5.83 (m, 1H); 4.44 – 4.41 (m, 2H); 4.27 (dd, *J* = 5.4, 4.2 Hz, 2H); 4.03 – 4.00 (m, 2H); 3.82 – 3.78 (m, 2H); 3.74 – 3.67 (m, 8H); 3.62 – 3.52 (m, 167H). ^{13}C NMR (125 MHz, $CDCl_3$): δ_C 130.96, 128.27, 70.53, 69.09, 63.67.

Section C. Nuclear Magnetic Resonance of Viologen Crosslinker and Photocatalysts (^{1}H)

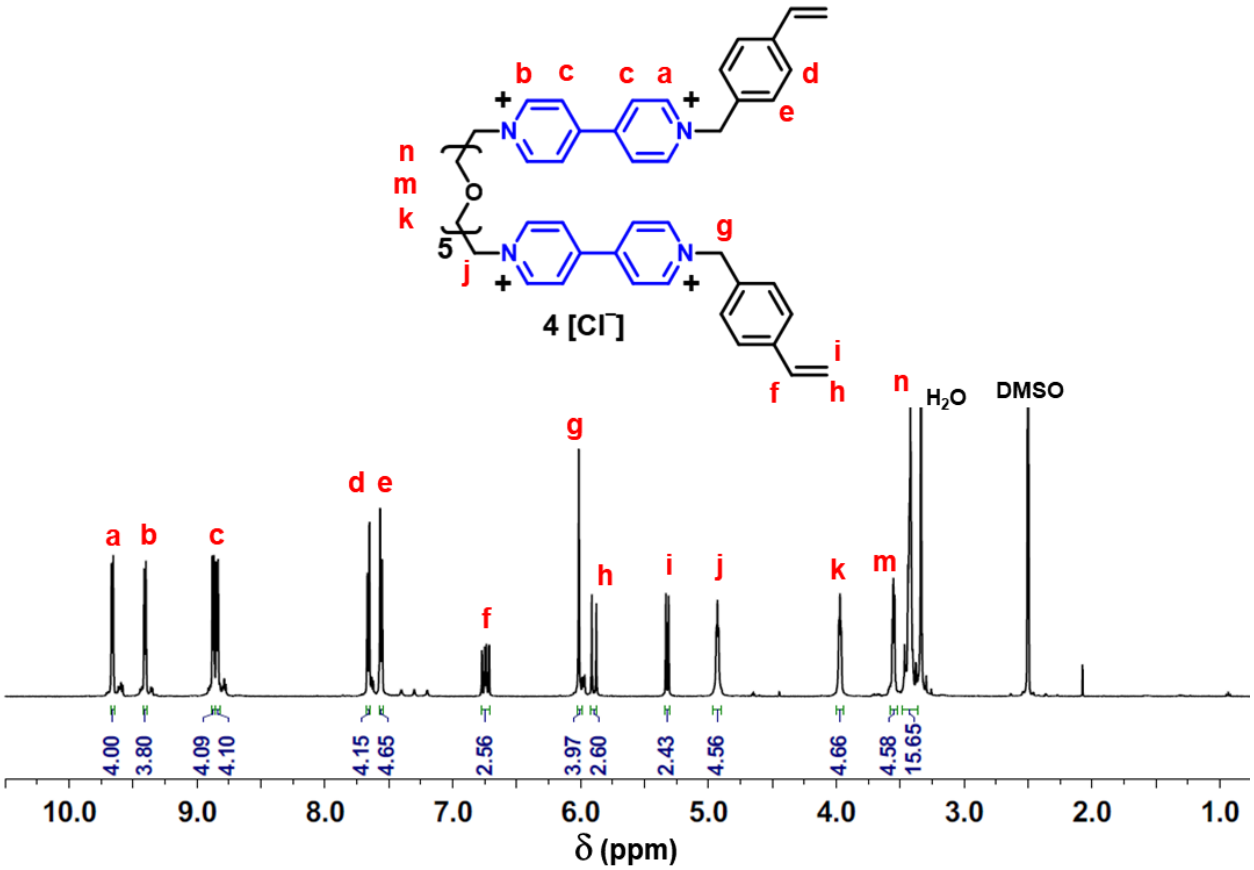

Figure S1: ^{1}H NMR (500 MHz, $(CD_3)_2SO$) spectra for the **2V-St** • 4Cl crosslinker used in the synthesis of microparticles.

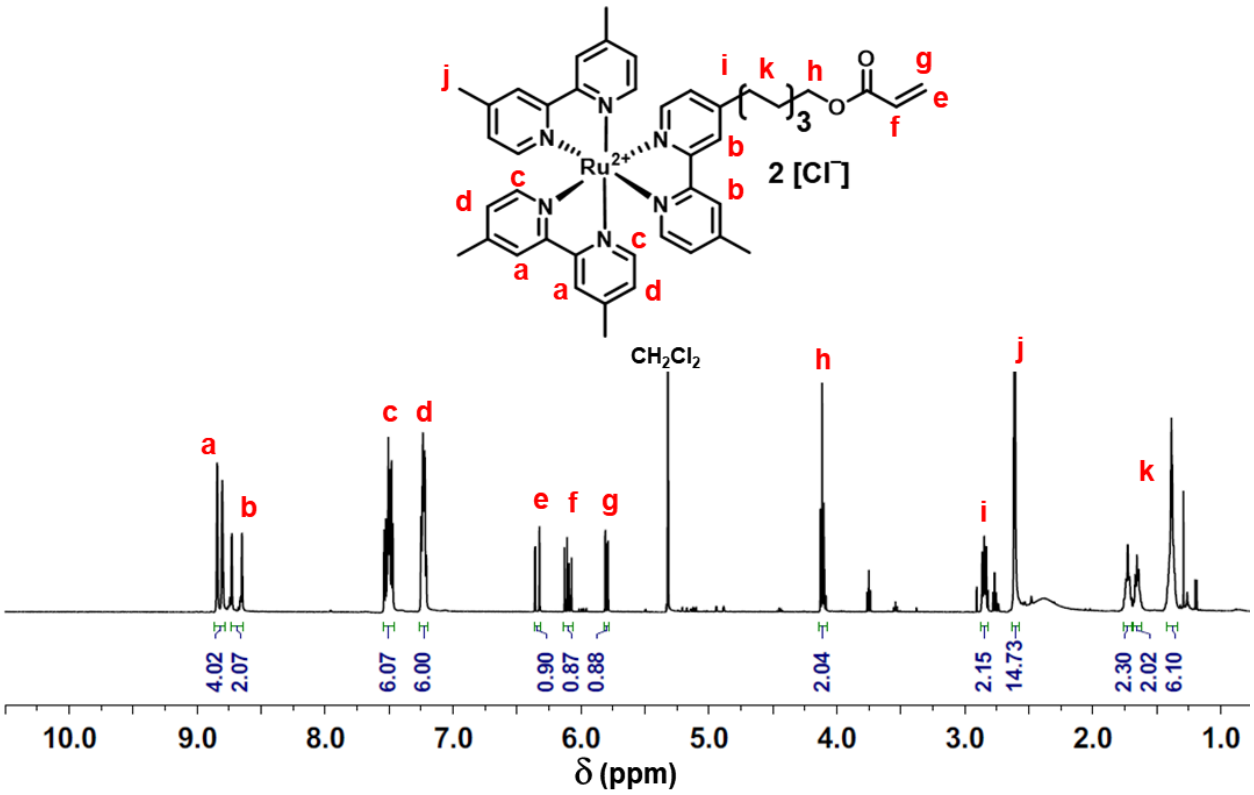

Figure S2: ^{1}H NMR (500 MHz, CD_2Cl_2) spectra for **Ru(bpy)$_3$ Ac** used in the synthesis of microparticles.

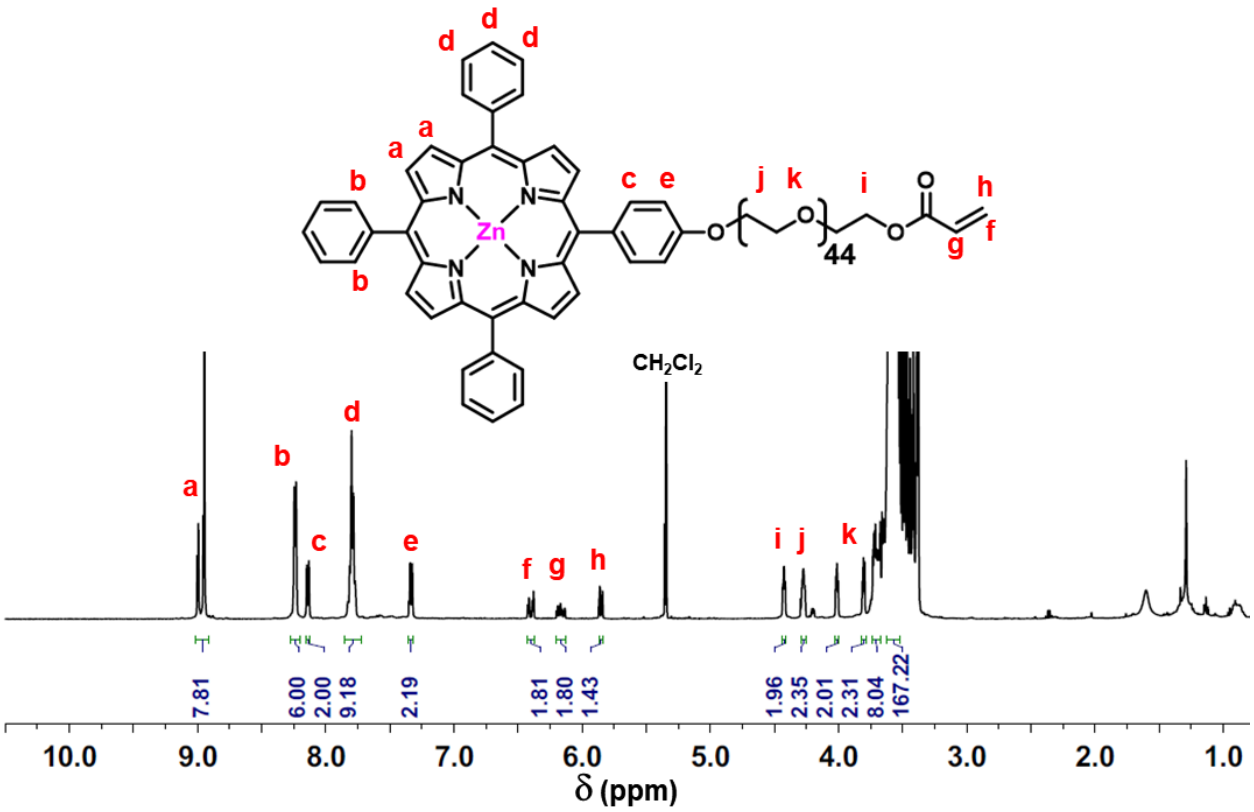

Figure S3: ^{1}H NMR (500 MHz, CD_2Cl_2) spectra for **ZP−PC** pendent used in the synthesis of microparticles.

Section D. Microparticle Preparation / Reduction Tests / Electrostatic Loading

1) General Procedure for the Preparation of Zinc Porphyrin Microparticles (MP-1)

Oil	Aqueous								Emulsifier	Initiator	
Oil (mL)	PEGDA (mg)	PEGDA (mmol)	PEGDA (μL)	V XL (mg)	V XL (mmol)	Photocat (mg)	Photocat (mmol)	H_20 (μL)	PGPR (mg)	APS (mg)	APS (mmol)
1.80	25.0	0.043	22.3	50.0	0.053	3.947	0.00144	200.0	78.3	2.368	0.010

Table S1: Reagents used for the synthesis of **MP-1** crosslinked with **(3)**.

Microparticles were prepared in batches through a water-in-oil (W/O) emulsion method utilizing vegetable oil, aqueous reagents listed in **Table S1**, polyglycerol polyricinoleate (PGPR) emulsifier, and an aqueous initiator, ammonium persulfate (APS). **(3), (14),** polyethylene glycol diacrylate (PEGDA) (M_W 575) and APS were dissolved in deionized H_2O in a small scintillation vial. The oil layer composed of vegetable oil and PGPR emulsifier was added to a separate vial. The aqueous vial was mixed and sonicated for 2 min to ensure complete solubility. The contents were then transferred to the vial containing the oil layer by micropipette. The vial was vortexed for one minute to ensure thorough emulsion formation. The vial was placed into an 80 °C oven for 1 h to ensure complete polymerization. After polymerization, the product mixture was washed into a 15 mL centrifuge tube with hexanes and diluted up to 15 mL with hexanes. The mix was centrifuged at 3000 rpm at -10°C for 10 min. The supernatant was decanted away, and the pellet was washed again with 15 mL of hexanes followed by centrifugation. The pellet was then washed with 15 mL MeOH to wash away unreacted reagents. The mix was centrifuged at 4000 rpm at -10°C for 15 min. The supernatant was decanted away, and the pellet was washed again with 15 mL of MeOH followed by centrifugation. The supernatant was decanted away yielding **MP-1** (50 mg, 61% mass yield). To calculate the yield for each batch, the microparticles were taken up in MeOH to an exact volume of 10 mL and mixed well to a thorough suspension. A 500 μL aliquot was taken and transferred to a pre-tared vial. The vial was dried under vacuum and the aliquot mass was obtained. The total for the batch yield was then calculated by multiplying the aliquot mass by a factor of 20. A separate 500 μL aliquot was taken for optical microscopy, scanning electron microscopy (SEM), and dynamic light scattering (DLS) analysis. The remaining fraction of the microparticle batch (18/20th) of the total mass, was carried forward to loading with methyl orange dye anion.

2) General Procedure for the Preparation of Ru(bpy)$_3$ Microparticles (MP-2)

Oil	Aqueous								Emulsier	Initiator	
Oil (mL)	PEGDA (mg)	PEGDA (mmol)	PEGDA (μL)	V XL (mg)	V XL (mmol)	Photocat (mg)	Photocat (mmol)	H_20 (μL)	PGPR (mg)	APS (mg)	APS (mmol)
1.80	25.0	0.043	22.3	50.0	0.053	1.258	0.00143	200.0	78.3	2.288	0.010

Table S2: Reagents used for the synthesis of **MP-2** crosslinked with **(3)**.

Microparticles were prepared in batches through a water-in-oil (W/O) emulsion method utilizing vegetable oil, aqueous reagents listed in **Table S2**, PGPR emulsifier, and an aqueous initiator APS. **(3), (9)**, PEGDA (M_W 575) and APS were dissolved in deionized H_2O in a small scintillation vial. The oil layer composed of vegetable oil and PGPR emulsifier was added to a separate vial. The aqueous vial was mixed and sonicated for 2 min to ensure complete solubility. The contents were then transferred to the vial containing the oil layer by micropipette. The vial was vortexed for one minute to ensure thorough emulsion formation. The vial was placed into an 80 °C oven for 1 h to ensure complete polymerization. After polymerization, the product mixture was washed into a 15 mL centrifuge tube with hexanes and diluted up to 15 mL with hexanes. The mix was centrifuged at 3000 rpm at -10°C for 10 min. The supernatant was decanted away, and the pellet was washed again with 15 mL of hexanes followed by centrifugation. The pellet was then washed with 15 mL MeOH to wash away unreacted reagents. The mix was centrifuged at 4000 rpm at -10°C for 15 min. The supernatant was decanted away, and the pellet was washed again with 15 mL of MeOH followed by centrifugation. The supernatant was decanted away yielding **MP-2** (40 mg, 51% mass yield). To calculate the yield for each batch, the microparticles were taken up in MeOH to an exact volume of 10 mL and mixed well to a thorough suspension. A 500 μL aliquot was taken and transferred to a pre-tared vial. The vial was dried under vacuum and the aliquot mass was obtained. The total yield for the batch was then calculated by multiplying the aliquot mass by a factor of 20. A separate 500 μL aliquot was taken for optical microscopy, scanning electron microscopy (SEM), and dynamic light scattering (DLS) analysis. The remaining fraction of the microparticle batch (18/20th) of the total mass, was carried forward to loading with methyl orange dye anion.

3) Photochemical Reduction of Microparticles

To test for the presence of and the effectiveness of the viologen subunits within the microparticles to reduce via photo-irradiation, **MP-1** and **MP-2** batches were synthesized as described in section D1, D2 with **(3)** and PEGDA in two different **(3)** wt : PEGDA wt % ratios (**Table S3**). Aliquots were suspended in approximately 2 mL of a 3 mM solution of triethanolamine (TEOA) in H_2O in a 2-dram scintillation vial. In an inert glovebox atmosphere of UHP nitrogen, the vials were placed between two desk lamps equipped with blue aquarium LED lightbulbs to irradiate at 450 nm for 60 min. Before (**Figure S4 left**) and after (**Figure S4 right**) images were taken, and the vials were observed to have changed colour, which is indicative of photoreduction of the viologen units within the microparticles. This result was expected due to the reported redox potentials of Zn porphyrins, TEOA, and oligoviologen dimers.[6,7] The redox potentials of water soluble ^{3}Zn porphyrin*, ($ZnTPP^+/^3ZnTPP^*$) and ($^3ZnTPP^*/ZnTPP^-$), were reported to be –0.75 V and 0.45 V (vs Ag/AgCl), respectively.[6] The oxidation potential of TEOA is 0.87 V (vs Ag/AgCl). The two reduction potentials of HEG-spaced oligoviologens were reported to be –0.43 and –0.96 V (vs Ag/AgCl), respectively.[7]

Microparticle Batch	2V-St • 4Cl : PEGDA wt % ratio
ZB (MP-1)	3:1
ZC (MP-1)	2:1
RB (MP-2)	3:1
RC (MP-2)	2:1

Table S3: Microparticle batch compositions tested by photochemical and chemical reduction.

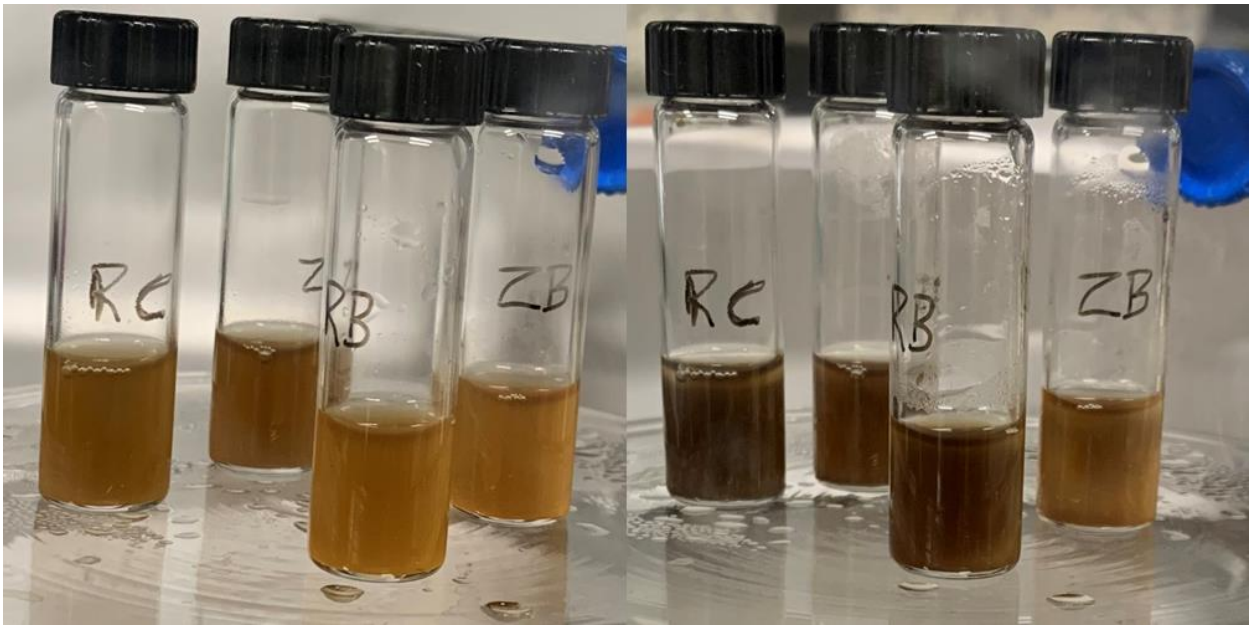

Figure S4: Pictures of microparticle vials before (left) and after 60 min (right) irradiation with blue light.

4) Chemical Reduction of Microparticles

To test for the presence of and effectiveness of the viologen subunits within the microparticles to reduce via chemical reduction, aliquots from the same **MP-1** and **MP-2** batches were taken up in approximately 2 mL of H_2O in a 2-dram scintillation vial. A picture was taken of the microparticle suspension in the vials (**Figure S5 Top**). To the vials, 1 mL of 0.1 M sodium dithionite ($Na_2S_2O_4$) solution in H_2O was added by syringe. Immediately, the microparticles turned a dark purple colour which is indicative of chemical reduction of the viologen subunits within the microparticles (**Figure S5 Middle**). To prove the purple colour was present only within the microparticles themselves, the reduced microparticles filtered through a 0.45 μm filter. After filtration, the filtrate was clear (**Figure S5 Bottom**), indicating there was no unpolymerized, reduced viologen present in the solution. To further corroborate chemical reduction, the microparticles were plated onto a small (35 mm diameter) Falcon polystyrene petri dish and observed by optical microscope (**Figure S6 Left**). A few drops of 0.1 M sodium dithionite were placed into the petri dish solution to reduce the microparticles, evident by the drastic colour change observed (**Figure S6 Right**).

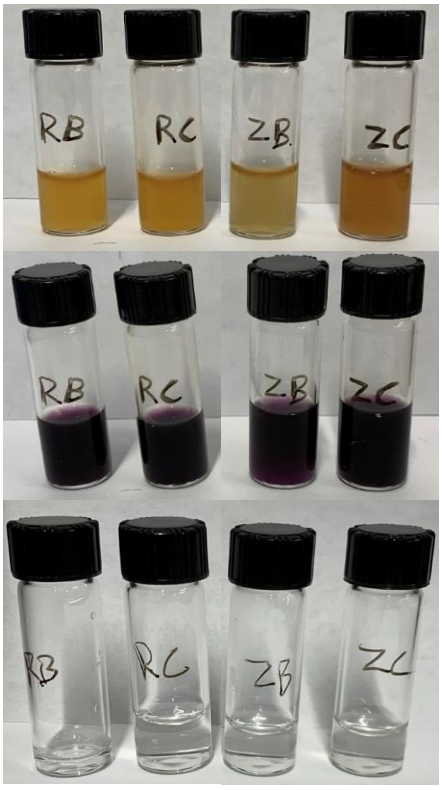

Figure S5: Pictures of microparticle vials before (top) and after (middle) chemical reduction with $Na_2S_2O_4$. Clear filtrate of reduced microparticles (bottom).

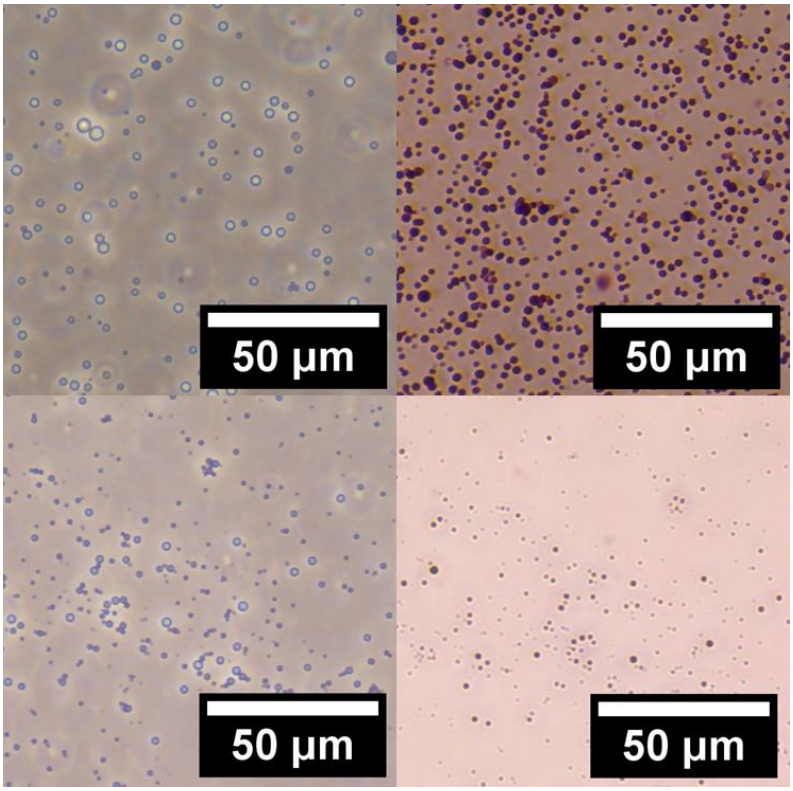

Figure S6: Optical microscopy pictures of microparticles before (left) and after (right) chemical reduction with $Na_2S_2O_4$.

5) Small Molecule Methyl Orange Loading

To demonstrate that MO can be properly loaded onto the oligoviologen crosslinker within the microparticle, a small-molecule test was conducted. **(3)** (50 mg, 0.053 mmol, 1 equiv) was dissolved in approximately 3 mL H_2O. MO (175 mg, 0.53 mmol, 10 equiv) was dissolved in approximately 15 mL H_2O. The two aqueous solutions were combined into a 50 mL centrifuge tube resulting in a precipitation of an orange solid. The mix was centrifuged at 4500 rpm at -10 °C for 10 minutes. The supernatant was discarded, and the solid precipitate was washed again with H_2O. The mix was centrifuged again at 4500 rpm at –10 °C for 10 minutes. This process was repeated several times until the aqueous supernatant was very pale in colour. The pellet was dried by lyophilizer to yield a red-orange solid (75 mg, 70% yield). The ^{1}H NMR spectrum of the solid was compared to **(3)** and MO starting material (**Figure S7**) to show the successful counteranion exchange of four methyl orange moieties for one oligoviologen crosslinker.

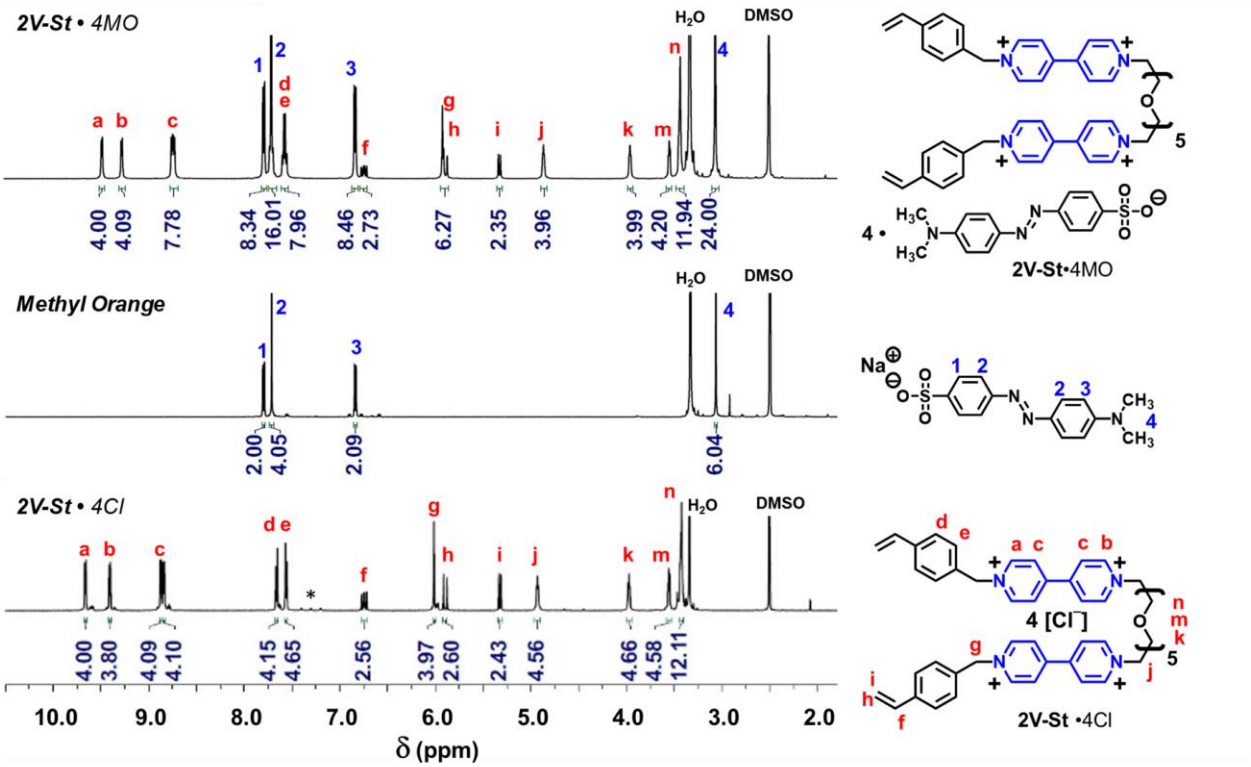

Figure S7: ^{1}H NMR (500 MHz, $(CD_3)_2SO$) spectra showing small molecule counteranion exchange/loading of MO onto **2V-St** • 4Cl to yield **2V-St** • 4MO. * Trace NH_4PF_6 from synthesis of **2V-St** • 4Cl washed away during loading of MO.

MO is known to have large absorbance at 450 nm. To assert that MO cannot serve as a photocatalyst for reduction of oligoviologens during irradiation, and to assess the loading of MO on higher molecular weight oligoviologen crosslinkers, **6V-St** • 12Cl was dissolved in approximately 3 mL H_2O. MO was dissolved in

approximately 15 mL H_2O. The two aqueous solutions were combined into a 50 mL centrifuge tube resulting in a precipitation of an orange solid. The mix was centrifuged at 4500 rpm at –10 °C for 10 minutes. The supernatant was discarded, and the solid precipitate was washed again with H_2O. The mix was centrifuged again at 4500 rpm at –10 °C for 10 minutes. This process was repeated several times until the aqueous supernatant was very pale in colour. The pellet was dried by lyophilizer to yield a red-orange solid. The ^1H NMR spectrum of the solid was compared to the oligoviologen starting material and MO starting material (**Figure S8**) to show the successful counteranion exchange of 12 MO moieties for one oligoviologen crosslinker. The resultant MO-loaded oligoviologen in $(CD_3)_2SO$ was sparged with bubbling N_2 and transferred to a sealed glass NMR tube. The sample was analysed by NMR before and after 60 min irradiation with blue light. No change in the NMR peaks was observed, indicating no reduction of viologen subunits through irradiation of the MO-based salt.

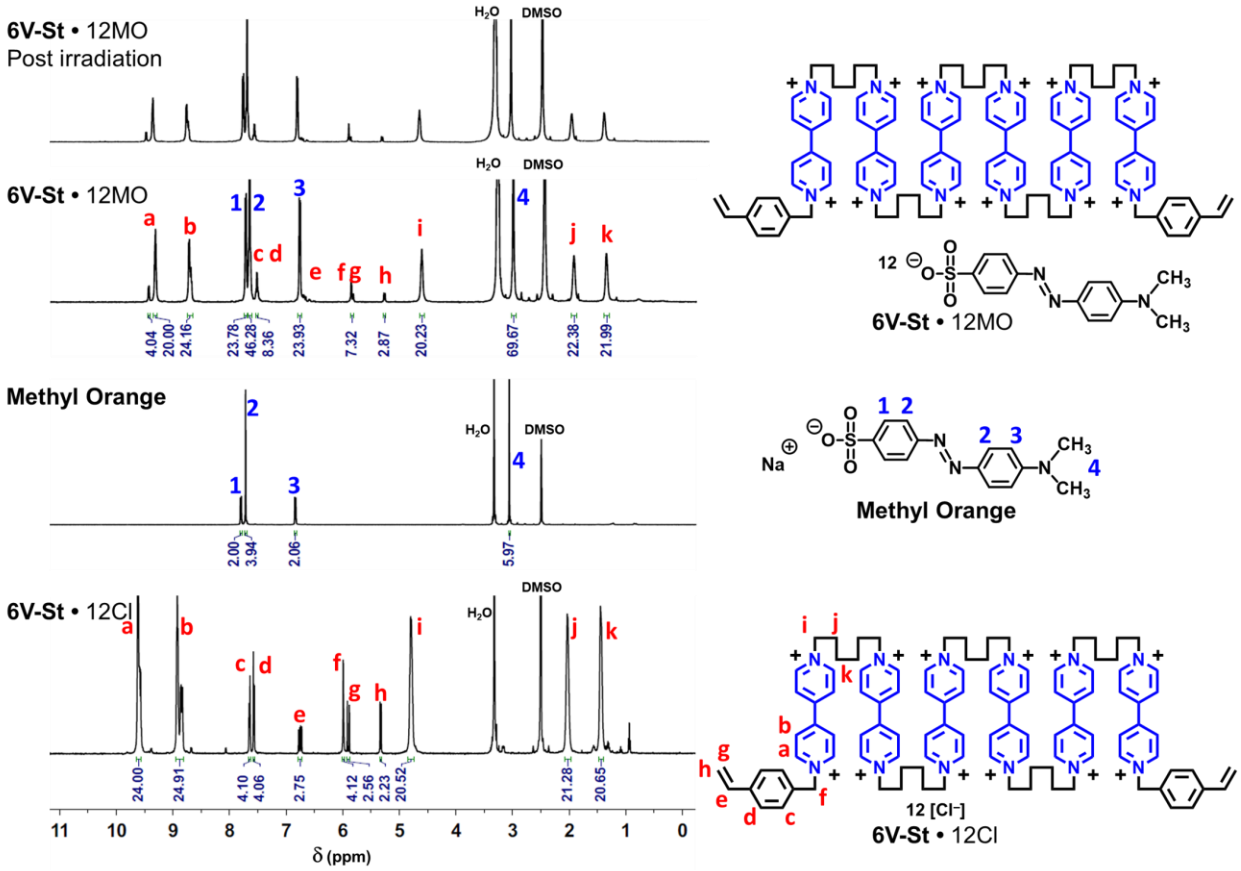

Figure S8: ^1H NMR (500 MHz, $(CD_3)_2SO$) spectra showing small molecule counteranion exchange/loading of MO onto **6V-St** • 12Cl to yield **6V-St** • 12MO.

6) Microparticle Loading of Methyl Orange

As-synthesized **MP-1** and **MP-2** batches were each obtained in triplicate. Controls for release kinetics tests were also synthesized in triplicate by systematically removing viologen crosslinker and photocatalyst from microparticle batches (**Table S4**). The microparticles were transferred to 8 dram scintillation vials as a suspension in approximately 5 mL MeOH. MO (200 mg) was added to a separate vial and dissolved in a 50:50 mix of MeOH:H_2O. The MO solution was poured into the scintillation vial containing the microparticles. The vial was sealed and placed on a shaker table at 90 rpm for 18 hours to ensure counteranion exchange. The microparticle batches were then transferred to 50 mL centrifuge tubes and the mix was centrifuged at 4500 rpm at -10 °C for 15 minutes. The supernatant was decanted and the microparticles were washed again with 50:50 MeOH:H_2O several times by centrifuge until the supernatant layer became very pale in colour. The microparticles were resuspended in MeOH to an exact volume of 10 mL and mixed well to a thorough suspension. To calculate the yield for each batch, a 500 μL aliquot was taken and transferred to a pre-tared vial. The vial was dried under vacuum and the aliquot mass was obtained. The total yield of the batch was then calculated by multiplying the aliquot mass by a factor of 20. A separate 500 μL aliquot was taken for optical microscopy, SEM, and DLS analysis. The MO-loaded microparticles (**MP-1** and **MP-2**) were analysed by optical microscopy and were compared to the as-synthesized precursors **(Figure S9)**. The MO-loaded **MP-1** microparticles were observed to aggregate together much more than the as-synthesized microparticles. The MO-loaded **MP-2** microparticles were clumped and aggregated such that they could not be well analysed by optical microscopy and ImageJ **(Figure S8, top)**. For this reason, **MP-2** microparticles were not taken forward to further characterization. The remaining fraction of the **MP-1**, **MP-3**, and **MP-4** batches (18/20th of the total mass), were carried forward to dye release testing.

Sample/Control (each in triplicate)	Viologen Crosslinker	Photocatalyst
MP-1	Y	Y (Zn)
MP-2	Y	Y (Ru)
MP-3	Y	N
MP-4	N (PEGDA only)	Y (Zn)
MP-1_No-hν	Y	Y (Zn)

Table S4: Reagents included in each microparticle and control batch.

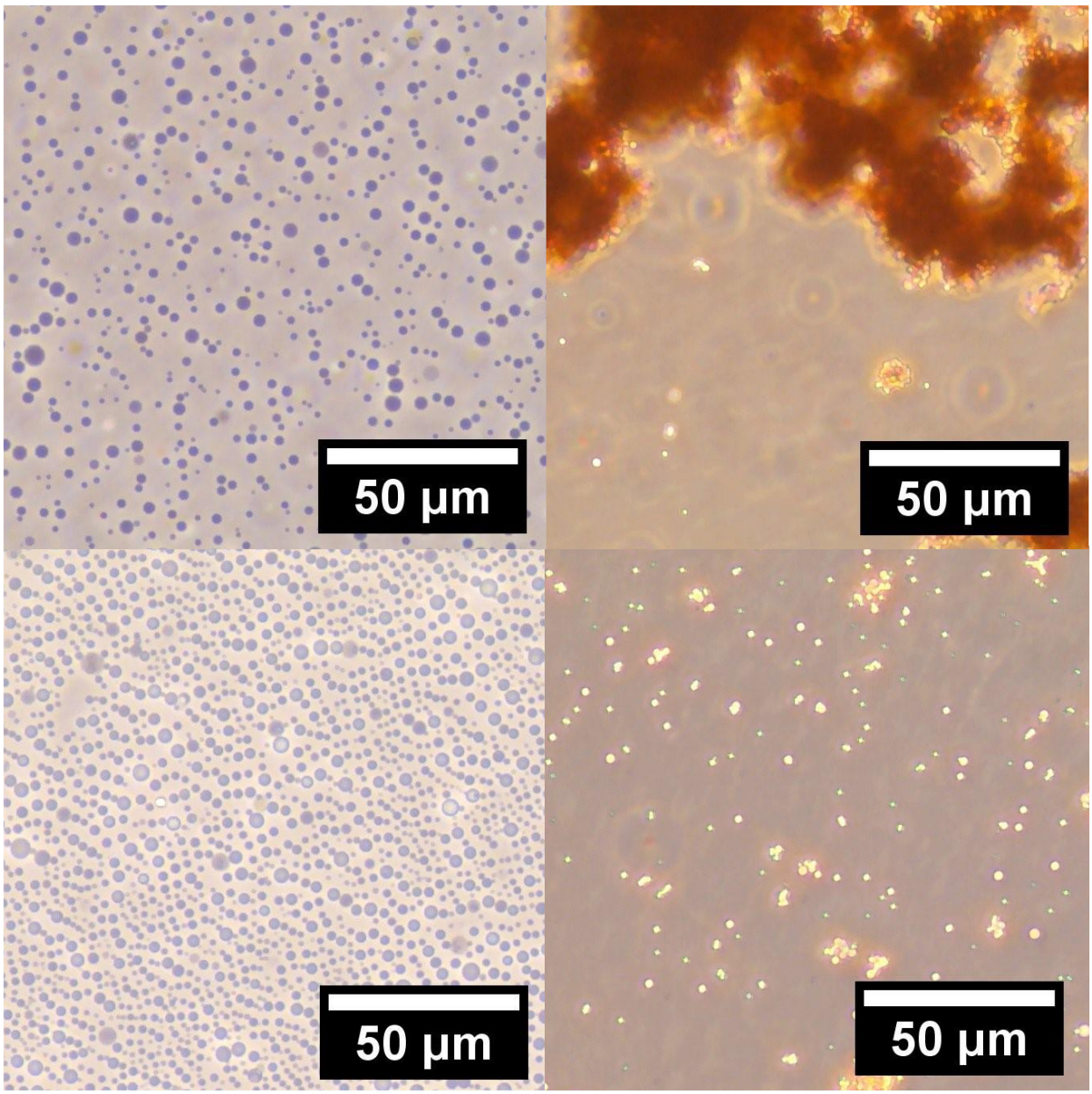

Figure S9: Zoomed-in optical microscopy pictures of microparticles before (left) and after (right) loading of MO. Top: **MP-2** Bottom: **MP-1**.

7) Loading Capacity Calculation

To calculate the loading capacity of anionic cargo per mg of microparticles, the viologen composition of the microparticles needed to be quantified. First, the theoretical mass percentage of nitrogen was calculated (**Figure S10, Eq. S1-S6**) based on the reagents used in **Table S1**. Elemental analysis was then performed to measure an actual mass percentage of nitrogen (**Figure S10, Eq. S7**). It was calculated that the theoretical N content in the as-synthesized and loaded particle is 3.78 wt% N and 8.67 wt% N respectively. Elemental analysis of the microparticles measured N content of 3.07 wt% and 8.26 wt% respectively. The measured mass percentage of nitrogen was compared to the theoretical mass percentage of nitrogen to evaluate what fraction of nitrogen-containing species were included in the polymerization (N_{frac}) (**Figure S10, Eq. S8**). The calculated fraction was then multiplied by the theoretical molar amounts of **2V-St** • 4Cl to determine the post-polymerization molar quantity (**Figure S10, Eq. S9**). We assumed that PEGDA and APS inclusion into the post-polymerization batch proceeded with the same fraction. The post-polymerization theoretical yield of microparticles was calculated (**Figure S10, Eq. S10**). Because there are 4 cargo loading sites per viologen chain, the micromole loading capacity was calculated (**Figure S10, Eq. S11**) to be 2.623 μmol/mg of polymerized microparticles.

Compound	Label	Molecular Weight (g/mol)
ZP-PEG-Ac	$MW_{ZP\text{-}PEG\text{-}Ac}$	2730.55
2V-St • 4Cl	$MW_{\mathbf{2V\text{-}St}\bullet 4Cl}$	936.84
2V-St • 4MO	$MW_{\mathbf{2V\text{-}St}\bullet 4MO}$	2012.41
MO^-	MW_{MO}	304.34
N	MW_N	14.0

$$\text{Total Mass of Polymerizable MP Reagents } (m_T) = m_{PEGDA} + m_{\mathbf{2V\text{-}St}\bullet 4Cl} + m_{ZP\text{-}PEG\text{-}Ac} + m_{APS} \quad \text{Eq. S1}$$
$$m_T = 81.315 \text{ mg}$$

$$\text{Mass\% N in } \mathbf{2V\text{-}St}\bullet 4Cl\ (m\%_{NV}) = \frac{4 \times MW_N}{MW_{\mathbf{2V\text{-}St}\bullet 4Cl}} \times 100 \quad \text{Eq. S2}$$
$$m\%_{NV} = 5.978\%$$

$$\text{Mass\% N in ZP-PEG-Ac } (m\%_{ZP}) = \frac{4 \times MW_N}{MW_{ZP\text{-}PEG\text{-}Ac}} \times 100 \quad \text{Eq. S3}$$
$$m\%_{ZP} = 2.051\%$$

$$\text{N Mass from } \mathbf{2V\text{-}St}\bullet 4Cl\ (N_V) = m\%_{NV} \times m_{\mathbf{2V\text{-}St}\bullet 4Cl} \quad \text{Eq. S4}$$
$$N_V = 2.989 \text{ mg N}$$

$$\text{N Mass from ZP-PEG-Ac } (N_{ZP}) = m\%_{ZP} \times m_{ZP\text{-}PEG\text{-}Ac} \quad \text{Eq. S5}$$
$$N_{ZP} = 0.081 \text{ mg N}$$

$$\text{Theoretical Mass\% N per Microparticle } (N_{ideal}) = \frac{N_{ZP} + N_V}{M_T} \times 100 \quad \text{Eq. S6}$$
$$N_{ideal} = 3.775\%$$

$$\text{Measured Mass\% N per Microparticle } (N_{meas}) = 3.07\% \quad \text{Eq. S7}$$

$$\text{Fraction of N-Containing Reagents Polymerized } (N_{frac}) = \frac{N_{meas}}{N_{ideal}} \quad \text{Eq. S8}$$
$$N_{frac} = 0.8132$$

$$\text{mmol of Viologen Post-Polymerization } (mmol'_V) = mmol_{\mathbf{2V\text{-}St}\bullet 4Cl} \times N_{frac} \quad \text{Eq. S9}$$
$$mmol'_V = 0.0434 \text{ mmol}$$

$$\text{Post-Polymerization Theoretical Loadable MP Yield } (m'_T) = N_{frac} \times (m_T) \quad \text{Eq. S10}$$
$$m'_T = 66.1254 \text{ mg}$$

$$\text{Anionic Cargo Loading Capacity of Unloaded MP (LC) } (\mu mol/mg) = \frac{4 \times mmol'_V}{m'_T} \times 1000 \quad \text{Eq. S11}$$
$$LC = 2.625 \ \mu mol/mg$$

Figure S10: Microparticle loading capacity calculation equations using elemental analysis

Section E. Microscopy / Light-Scattering / Release Kinetics Characterization

1) Optical Microscopy Imaging

Optical microscopy images were taken using a Thermo Fisher Scientific EVOS XL Core microscope with the 40x objective, 20/40 phase contrast filter, and a 3.1 megapixel camera. Microparticle samples were withdrawn from a well-mixed suspension with a glass pipette. H_2O was used to flush the microparticles out of the pipette into a small (35 mm diameter) Falcon polystyrene petri dish. The microparticles were allowed to settle to the bottom of the petri dish where they were photographed at a brightness between 80 and 85. The images were then opened within ImageJ software where a scale bar was established by first measuring a known distance between a pair of calliper tips and equating that distance to a measured number of pixels within the frame. The images were then saved with the scalebar generated in the bottom corner of the image.

2) Scanning Electron Microscopy (SEM) Imaging

Electron microscopy imaging was accomplished by SEM. Microparticles were synthesized as described in section D1. As-synthesized and loaded microparticles in a suspension of MeOH were drawn up and plated onto clean silicon wafers by glass pipette. The solvent was air dried, and the samples were then loaded into the SEM chamber. The sample chamber was evacuated using the HiVac setting, and images were recorded at 2,000x, 6,500x, 10,000x, 20,000x, and 65,000x magnification. The images **(Figure S11)** were then analysed using ImageJ software to calculate the size and distribution of the microparticles. At the highest magnifications, a corona morphology was observed in the microparticles, where the interior and exterior appear to have different densities. By measuring the inner and outer diameters with ImageJ (vide infra), the outer sphere corona volume was found to be 77.6 ± 5.85% of the total microparticle volume (**Figure S12**).

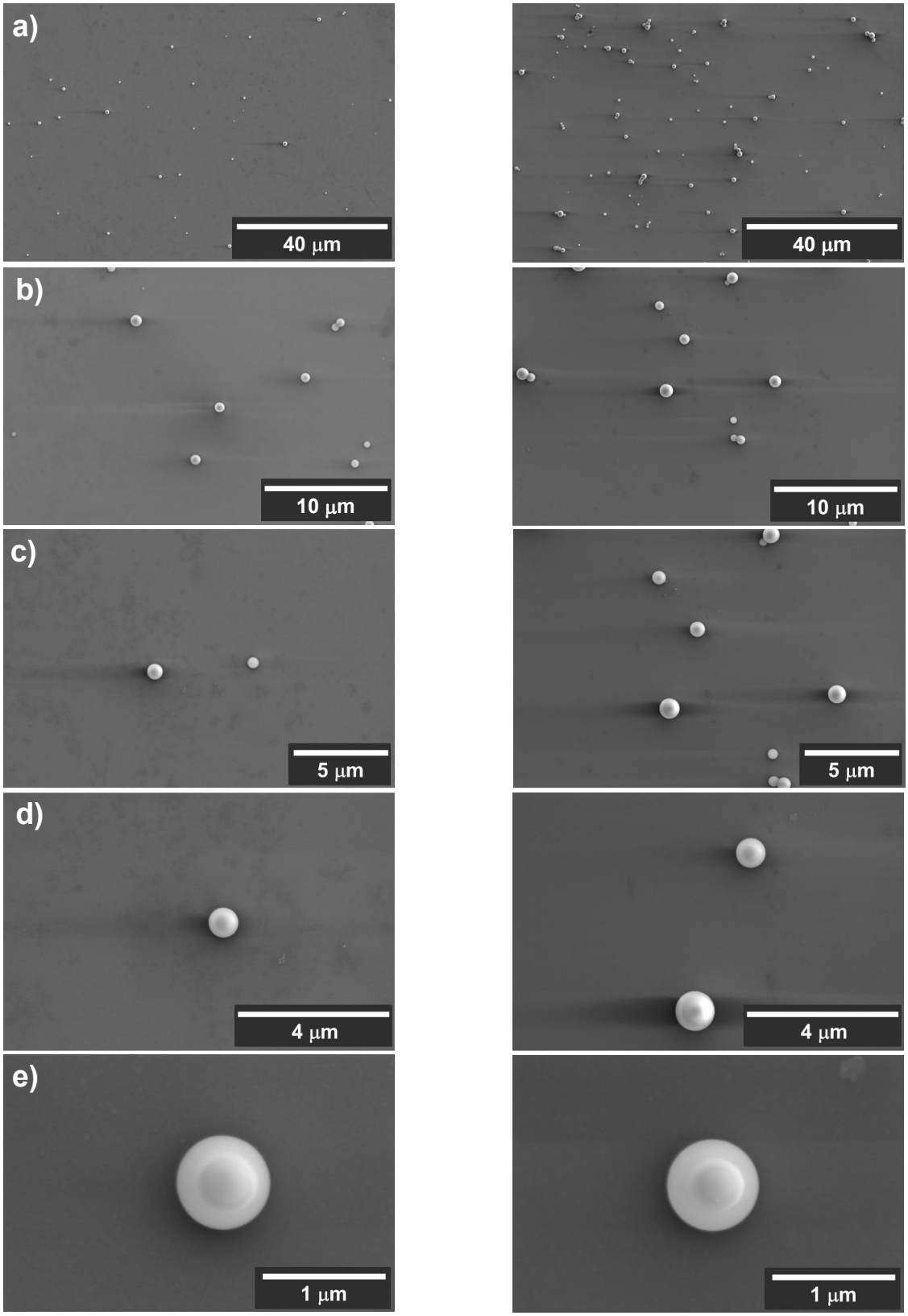

Figure S11: SEM images of microparticles before (left) and after (right) loading of MO. a) 2,000x, b) 6,500x, c) 10,000x, d) 20,000x, e) 65,000x magnification.

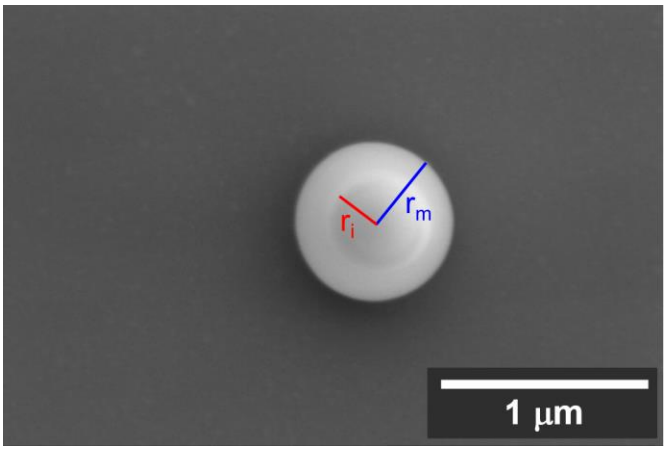

$$\text{Corona Volume \%} = \frac{\text{MP Volume} - \text{Inner Volume}}{\text{MP Volume}}$$

$$\text{Corona Volume \%} = \frac{\frac{4}{3}\pi r_m{}^3 - \frac{4}{3}\pi r_i{}^3}{\frac{4}{3}\pi r_m{}^3}$$

$$\text{Corona Volume \%} = 77.6 \pm 5.85$$

Figure S12: Evaluation of microparticle corona volumes using ImageJ.

3) ImageJ Analysis of Microscope Images

To establish size and distribution of the microparticles from the SEM images, three SEM image windows at 2,000x magnification were opened within ImageJ. The scale of the image was set accordingly, and the image type was set to 8-bit to generate a greyscale image. The RenyiEntropy threshold parameter was used to give well defined particle selection. The “close” and “fill holes” parameters were then used to allow for correction of light-centred or “hollow” appearing microparticles. The “watershed” function was used to divide partially overlapped microparticles. The microparticles were then analysed with the “exclude on edges” and “include holes” options marked as “true”, with a circularity of 0–1.00. The measurements of the data set were then taken, and the results were summarized as shown in **Table S5**.

Sample	Mean Diameter (μm)	Minimum Diameter (μm)	Maximum Diameter (μm)	Standard Deviation	Standard Error
As-Synthesized	0.481	0.139	1.695	0.278	0.0209
Loaded	0.785	0.151	2.521	0.362	0.0182

Table S5: Summary of microparticle measurements analysed by optical and scanning electron microscopy, measured by ImageJ software.

4) Dynamic Light Scattering Analysis of Microparticles

All light scattering experiments were performed in triplicate with 10 scans for each analysis. The individual number and intensity measurements during chemical reduction were plotted **(Figure 13a-c)**. The microparticles were prepared as described in section D1. 100 μL of a 2 $mg \cdot mL^{-1}$ suspension of microparticles in MeOH was diluted up to 1 mL with pure H_2O in a small scintillation vial. The suspension was well mixed before 200 μL of the diluted microparticle solution was deposited into three cuvettes. The microparticles were analysed one cuvette at a time by first measuring the as-synthesized size of the microparticles. The microparticles were then reduced by addition of 200 μL of 1M $Na_2S_2O_4$ solution in H_2O. Measurements were taken at 1, 3, 5, 15, and 30 min increments after addition of the dithionite. MO-loaded microparticles were also prepared as described in section D5, analysed, and plotted **(Figure S14)**. The average sizes of the microparticles for each time point were recorded (**Table S6**). The particles swelled in size in response to loading with a relatively large MO counteranion. During chemical reduction, the microparticles quickly exhibited a reduction in size to 471.933 ± 79.128 nm after 1 min before returning to their initial size and swelling slightly over the remaining timepoints. We hypothesize the swelling is due to a combination of factors. We speculate that counteranion metathesis replacing a small chloride counteranion with a larger dithionite counteranion that is abundant in solution results in swelling of the microparticle even while the viologen subunits are still reduced. We believe it is also due to the presence of ambient O_2 that re-oxidizes the viologen subunits within the microparticles. For this platform where the counteranion release is the critical component, it is not imperative to observe sustained physical contraction over the lifetime of microparticle reduction.

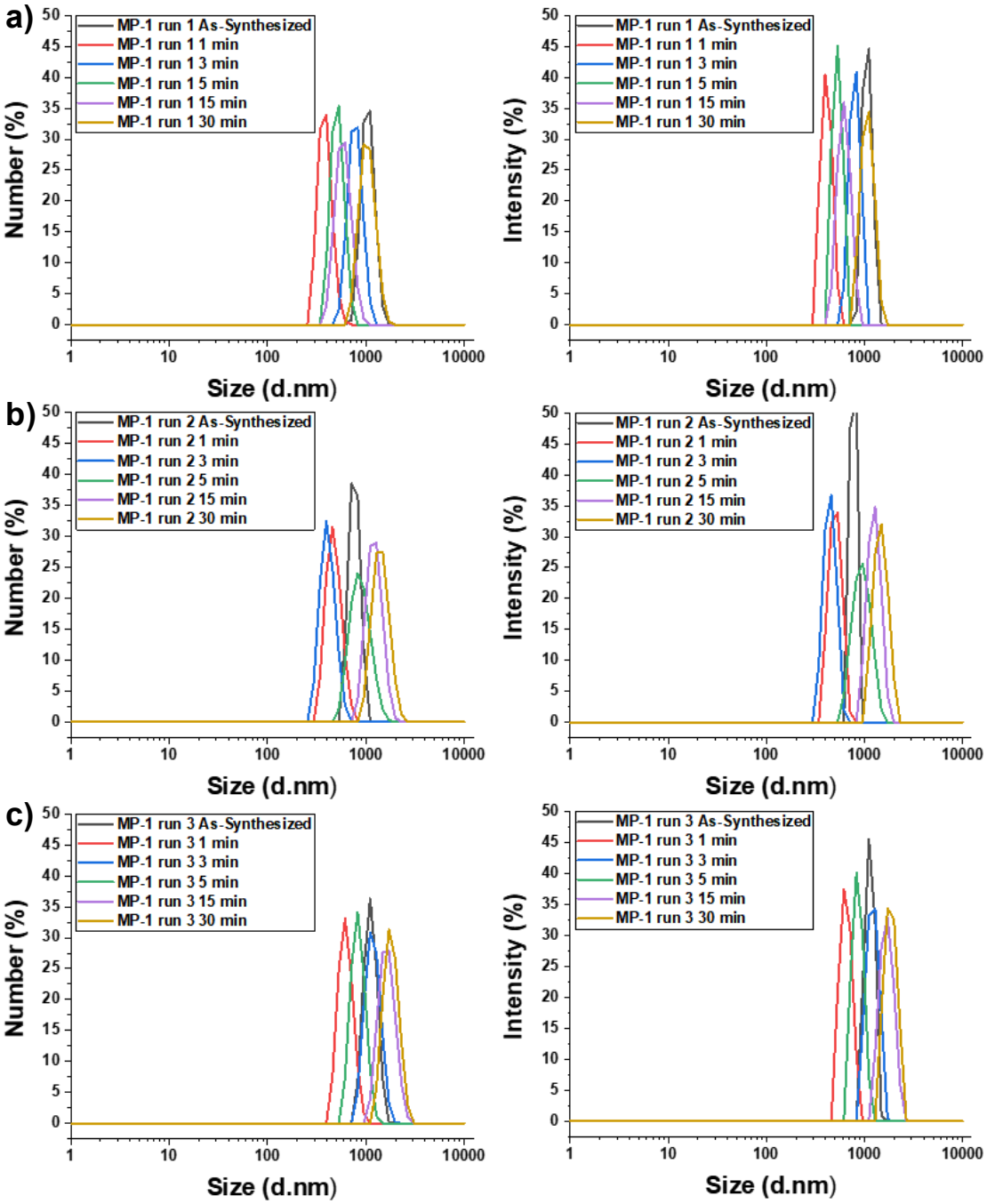

Figure S13: Dynamic light scattering traces (left: number, right: intensity) of microparticles before and during chemical reduction with $Na_2S_2O_4$. a) MP run 1, b) MP run 2, c) MP run 3.

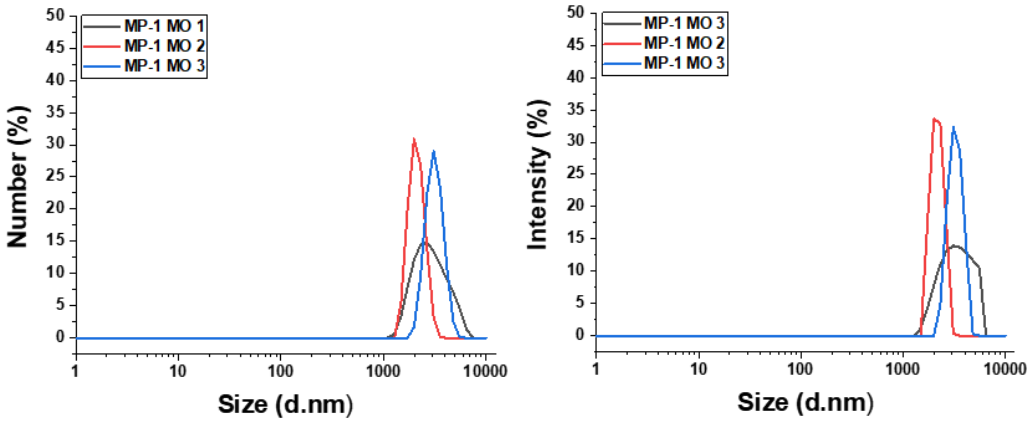

Figure S14: Dynamic light scattering traces (left: number, right: intensity) after loading with MO dye.

Sample	Number Mean Diameter (nm)	Intensity Mean Diameter (nm)
As-Synthesized	975.08 ± 93.814	1012.6 ± 93.814
1 min	471.93 ± 79.128	514.12 ± 39.038
3 min	834.13 ± 255.60	855.00 ± 237.96
5 min	727.05 ± 97.940	814.00 ± 125.46
15 min	1205.0 ± 320.78	1205.0 ± 262.42
30 min	1385.9 ± 225.66	1436.2 ± 178.28
Loaded	2688.2 ± 227.17	2724.0 ± 366.95

Table S6: Dynamic light scattering measured sizes of particles during chemical reduction and after loading.

5) Release Kinetics of Anionic Dye

To measure the release kinetics associated with the MO-loaded microparticles, sample and control microparticles were analysed in triplicate. **MP-1** microparticles (10 mg) were transferred in triplicate, as a suspension in MeOH, by micropipette to dialysis tubing. Control microparticles **MP-3**, **MP-4**, and **MP-1_No-hv** (10 mg each) were transferred in triplicate by the same method. The tubing was sealed with plastic dialysis clips and subsequently soaked in MilliQ H_2O for 36 h to dialyze any non-electrostatically bound MO. The MilliQ H_2O was exchanged several times where each subsequent wash became less coloured, indicating excess MO was successfully dialyzed away, and that no electrostatically bound MO was leaching out during washing. The dialysis tubing was then transferred to beakers containing 3 mM TEOA in MilliQ H_2O (500 mL). The samples were soaked in the TEOA solution for 3 h in the dark while 500 μL aliquots were taken for UV/Vis analysis. After 3 h, blue light was used to irradiate samples **MP-1**, **MP-3**, and **MP-4** for a period of up to 5 d, the point at which **MP-1** plateaued. **MP-1_No-hv** was kept in the dark by covering in foil for 5 d. Aliquots were taken from each batch and analysed by UV/Vis to track release throughout the irradiation. **MP-4** was tracked over only 48 h because there was no release observed. During the experiments, evaporation of H_2O was observed, so to account for the changing volume over time and to account for the volume taken in aliquots, the final volume of each beaker was measured with a graduated cylinder to facilitate calculation of the volume at each aliquot timepoint. In each release experiment, MO releases from the reduced viologen and diffuses away accompanied by the cation derived from the oxidized TEOA (radical cation). Such oxidized amines could potentially break down to generate iminiums which in turn can hydrolyse, providing protons. This process would lower the pH and potentially alter the conformation and electrostatic loading of the pH-sensitive MO dye. To test whether this is occurring during photo-triggered release of MO, the pH of the aliquots, post-irradiation, were compared to the pH of the 3 mM TEOA starting solution, and it was found to have no change (**Figure S15**). The lack of change is likely due to the large excess amount of unoxidized TEOA remaining in the aliquot solutions. The results indicate that such degradation is not occurring or that any small amount of degradation of the TEOA radical cation is not sufficient to significantly alter the pH, MO conformation, and the corresponding kinetic release results.

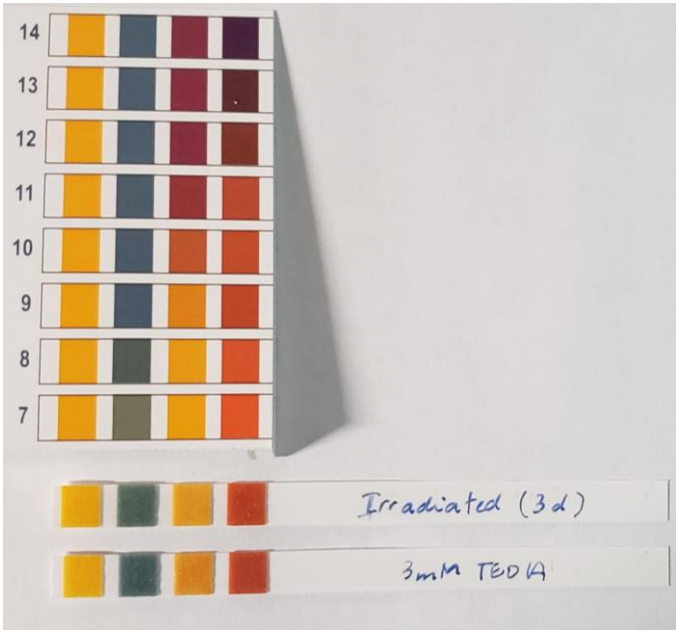

Figure S15: pH of post-irradiation aliquots compared to the 3 mM TEOA starting solution

To establish the maximum MO release capability of the microparticles, the mass fraction of MO anion within a loaded microparticle was determined. Because the theoretical and measured N content agreed so closely for the loaded particle, it was assumed that methyl orange counteranion metathesis of viologens in the polymerized microparticle was near quantitative. The molecular weight of the loaded viologen crosslinker (**2V-St** • 4MO) was used to establish the loaded viologen's mass contribution to the polymerized, loaded microparticle yield ($m'_{V\text{-}MO}$) (**Figure S16, Eq. S13**). The total polymerized mass contributions were then summed to give an expected batch yield of the microparticles once loaded (**Figure S16, Eq. S14**). The MO mass content and mass fraction MO of the microparticles were then calculated (**Figure S16, Eq. S15, S16**) yielding a mass fraction MO of 0.468. This mass fraction was then multiplied by the mass of microparticles added to each release kinetics experiment to determine the total mass and μmol release capability for methyl orange release from each experiment (**Figure S16, Eq. S17, S18**). The measured micromoles were then compared to the μmol release capability to establish percent release (**Figure S16, Eq. S19**).

$$\text{Mass of Viologen Post-Polymerization } (m'_V) = \text{mmol}' \times MW_{\mathbf{2V-St}\cdot 4Cl}$$
$$m'_V = 40.66 \text{ mg} \quad \text{Eq. S12}$$

$$\text{Mass of Viologen Post-Polymerization MO Loaded } (m'_{V\text{-}MO}) = \text{mmol}' \times MW_{\mathbf{2V-St}\cdot 4MO}$$
$$m'_{V\text{-}MO} = 87.34 \text{ mg} \quad \text{Eq. S13}$$

$$\text{Total Batch Mass of MO-Loaded MP Reagents } (m_{T\text{-}Load}) = m'_T - m'_V + m'_{V-MO}$$
$$m_{T\text{-}Load} = 112.81 \text{ mg} \quad \text{Eq. S14}$$

$$\text{Mass } MO^- \text{ per Batch } (m_{MO}) = 4 \times \text{mmol}'_V \times MW_{MO}$$
$$m_{MO} = 52.83 \text{ mg} \quad \text{Eq. S15}$$

$$\text{Mass Fraction } MO^- \text{ of Loaded Microparticles } (mfrac_{MO}) = \frac{m_{MO}}{m_{T-Load}}$$
$$mfrac_{MO} = 0.468 \quad \text{Eq. S16}$$

$$\text{Maximum mass } MO^- \text{ release from MP dye release experiment } (m_{max}) = mfrac_{MO} \times 10 \text{ mg}$$
$$m_{max} = 4.684 \text{ mg} \quad \text{Eq. S17}$$

$$\text{Maximum } \mu\text{mol } MO^- \text{ release from MP dye release experiment } (\mu mol_{max}) = \frac{m_{max}}{MW_{MO}} \times 1{,}000$$
$$\mu mol_{max} = 15.389 \ \mu\text{mol} \quad \text{Eq. S18}$$

$$\% \text{ Release} = \frac{\mu\text{mol measured}}{\mu mol_{max}} \quad \text{Eq. S19}$$

Figure S16: MO release capacity equations

6) UV/Vis Analysis of Dye Release

The aliquots taken from the release kinetics testing were analysed by a UV-Vis spectrophotometer. Each 500 μL aliquot was diluted up to 1 mL with pure MilliQ H_2O. The t=0 aliquot was used as a baseline reference and was corrected for in all other aliquots. The aliquots were then analysed within a window of 350 – 600 nm **(Figure S17-S28)**. The absorbance values at 465 nm were converted to a concentration value using a calibration curve formula obtained by measuring MO standards (**Figure S29)**. Concentration was then converted to micromoles released by using the volume at each aliquot timepoint. Loading capacity was calculated by using the wt% of MO (mg MO per mg loaded microparticle) multiplied by the total mass of microparticles in the dialysis tubing. Percent release was calculated by first comparing the measured micromoles released to the expected loading capacity micromoles of methyl orange, indicated by the black capacity line **(Figures S30, S31, S32)**. Because there was no expected loading capacity for **MP-4** due to the absence of viologens (and MO loading sites) within the microparticle, the measured micromoles released were compared to the expected loading of **MP-1 (Figure S33)**. Percent release vs time was then plotted. **(Figures S34, S35, S36, S37)**. To evaluate the effect of decreasing the TEOA concentration, release tests of **MP-1** and **MP-1_No-hv** were repeated where the microparticles were soaked in 0.3 mM TEOA while release was tracked across 5 d **(Figure S38)**. To investigate why MO release was plateauing at approximately 60-70%, a release test of **MP-1** was repeated, (**Figure S39**) but the TEOA solution was refreshed at 5 d with the exact volume of TEOA solution remaining at that time (indicated by dashed line). MO release was tracked for an additional 4 d until a new plateau was observed. The total release was calculated by summing the new release within the fresh TEOA solution with the total release from the initial solution.

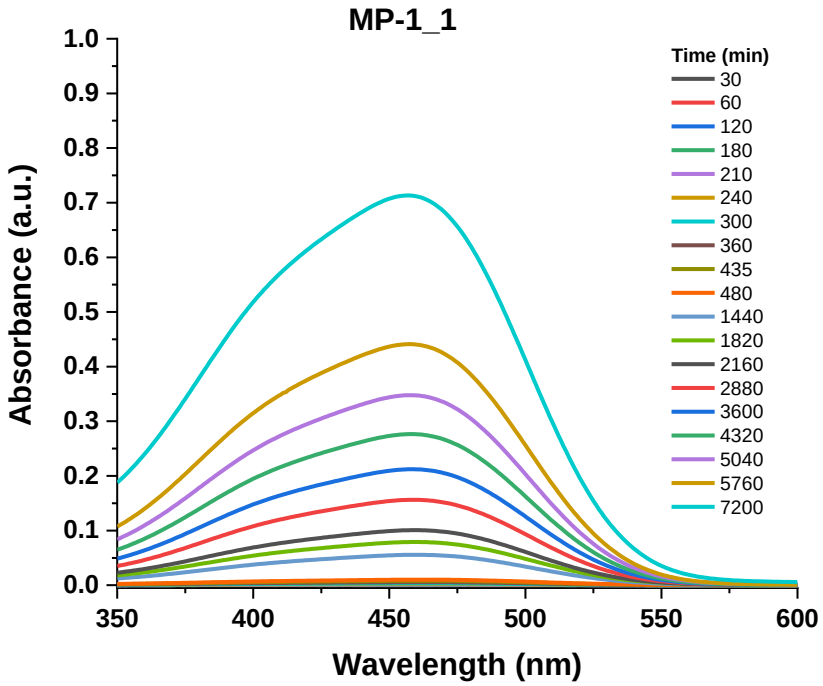

Figure S17: UV/Vis MO Release of MP-1_1

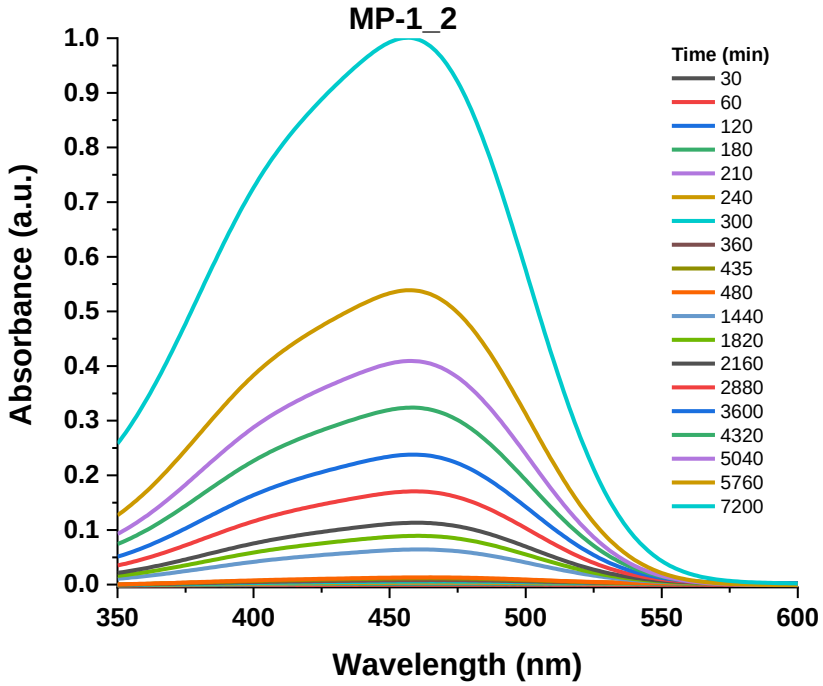

Figure S18: UV/Vis MO Release of MP-1_2

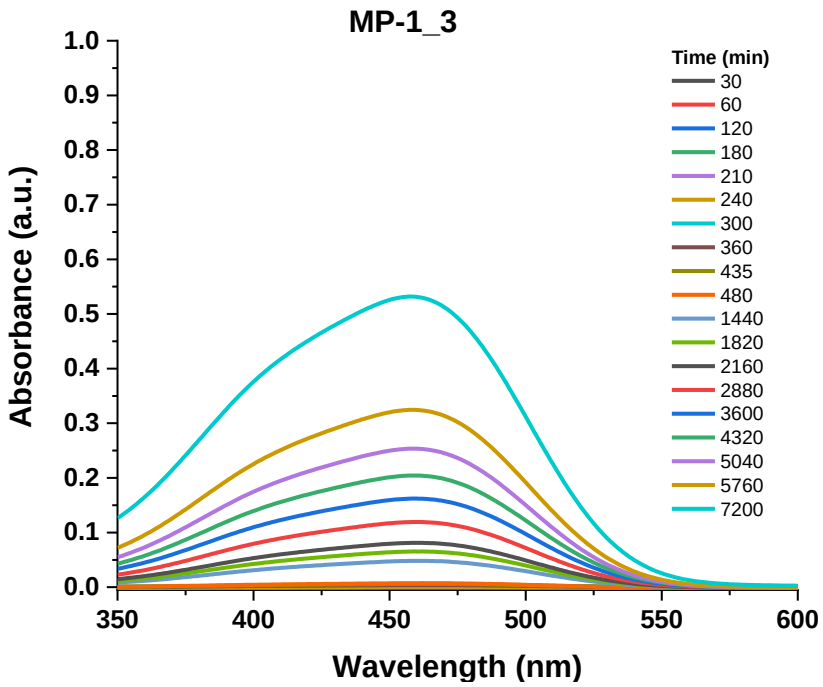

Figure S19: UV/Vis MO Release of MP-1_3

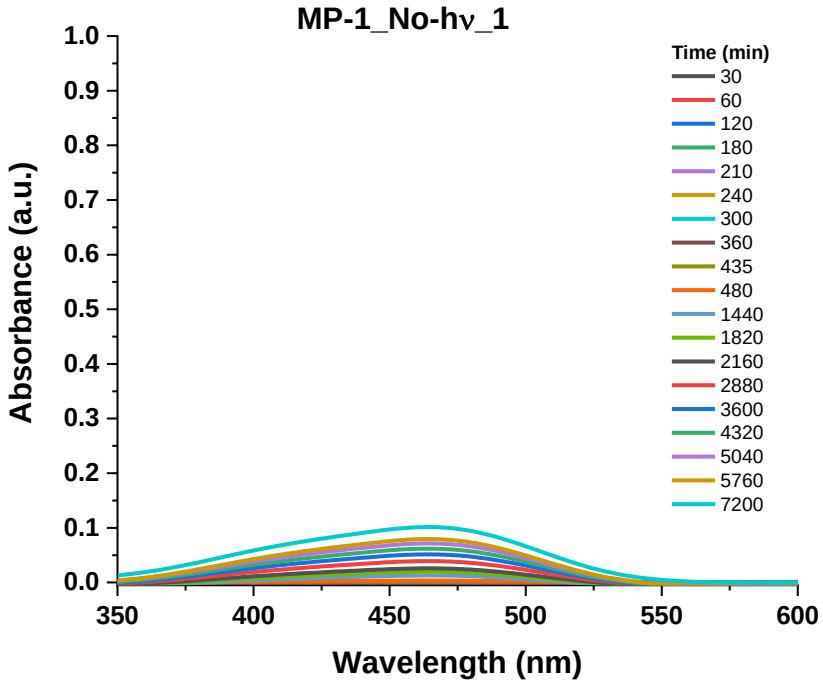

Figure S20: UV/Vis MO Release of MP-1_No-hv_1

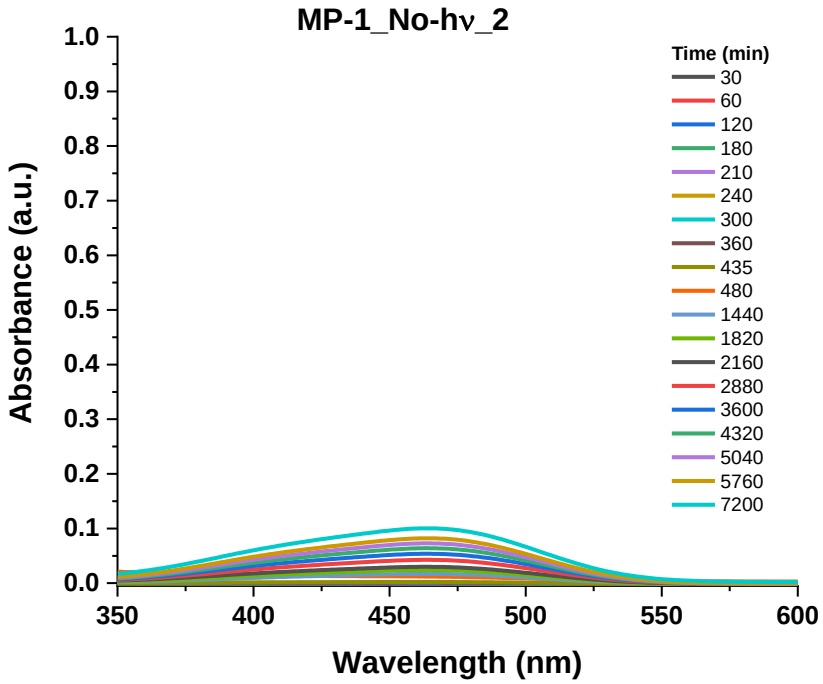

Figure S21: UV/Vis MO Release of MP-1_No-hv_2

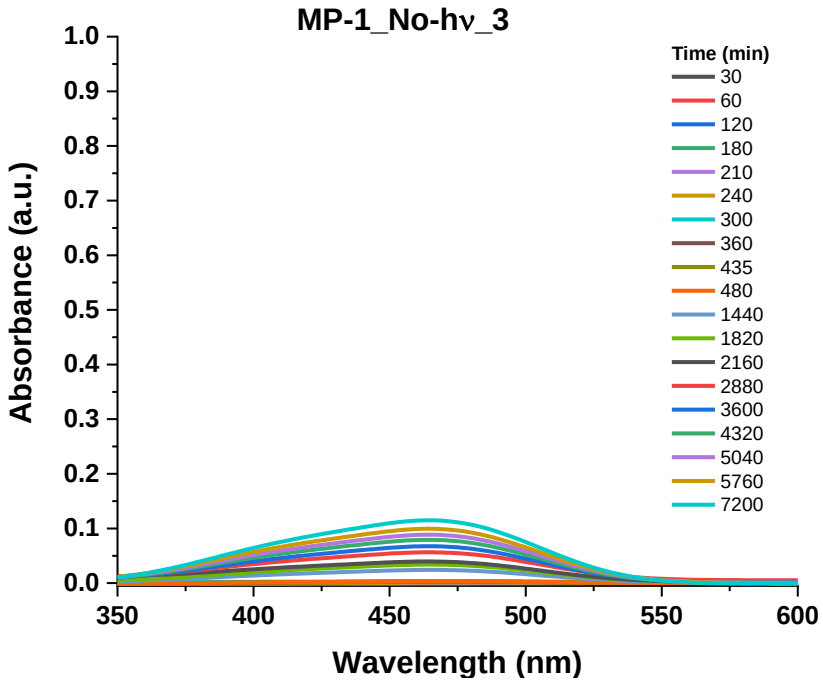

Figure S22: UV/Vis MO Release of MP-1_No-hv_3

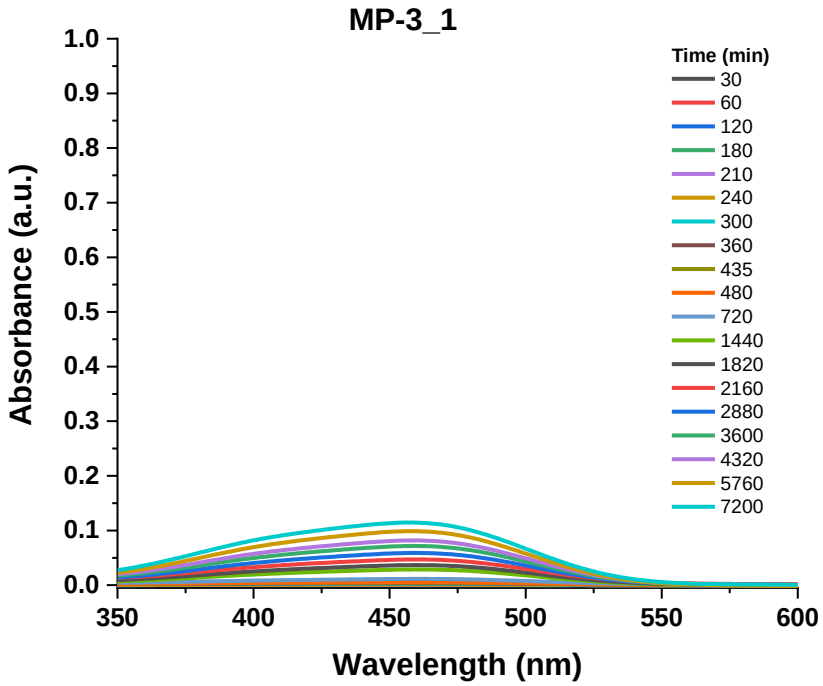

Figure S23: UV/Vis MO Release of MP-3_1

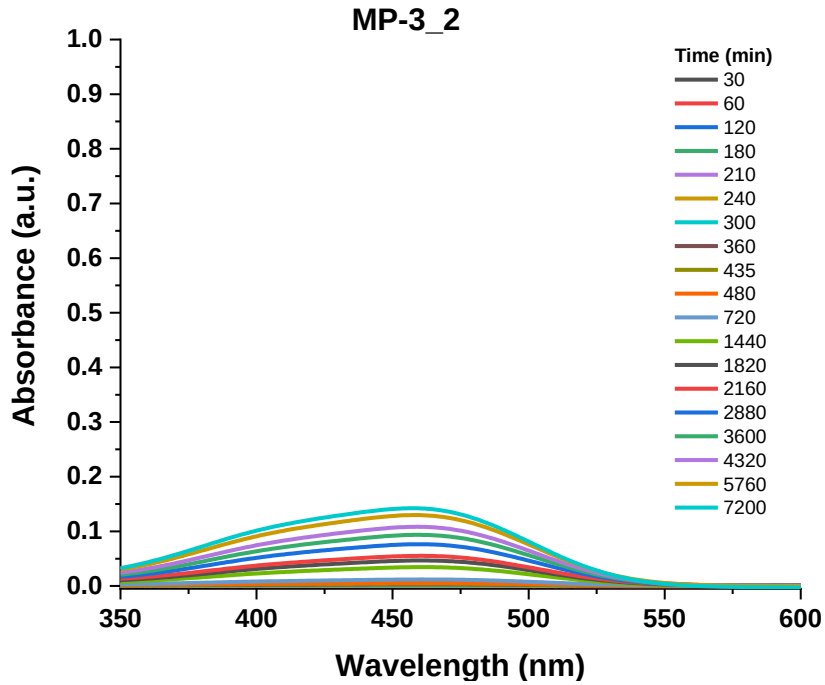

Figure S24: UV/Vis MO Release of MP-3_2

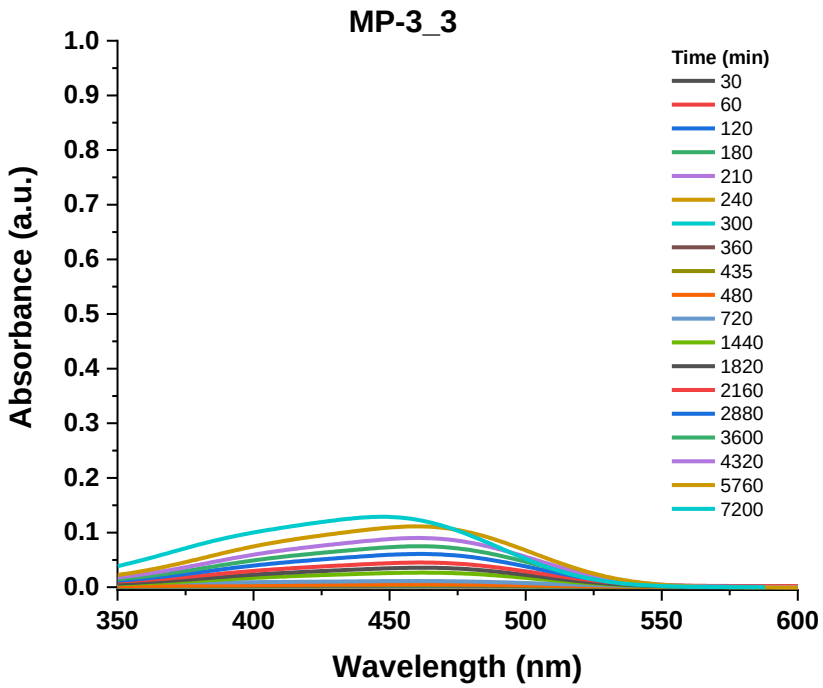

Figure S25: UV/Vis MO Release of MP-3_3

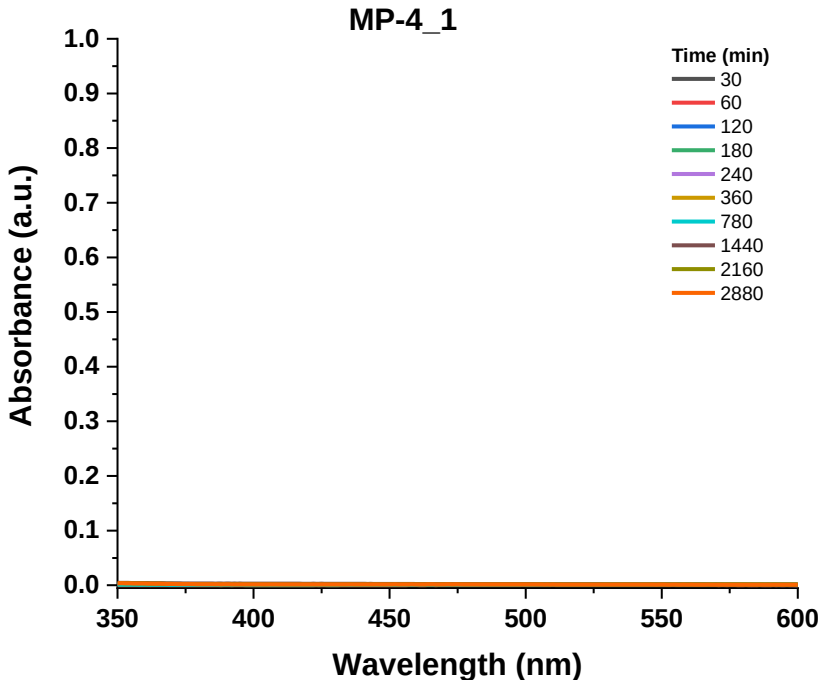

Figure S26: UV/Vis MO Release of MP-4_1

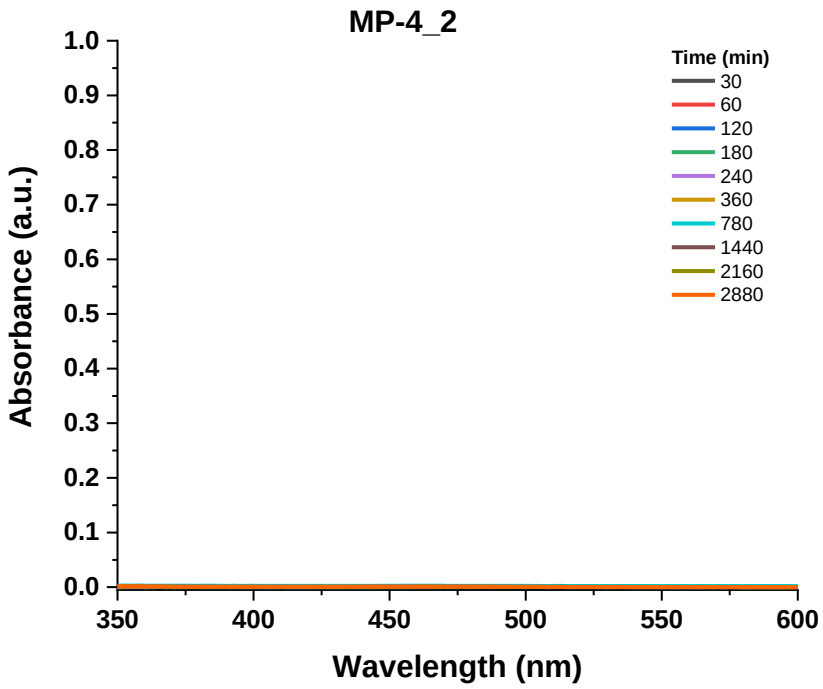

Figure S27: UV/Vis MO Release of MP-4_2

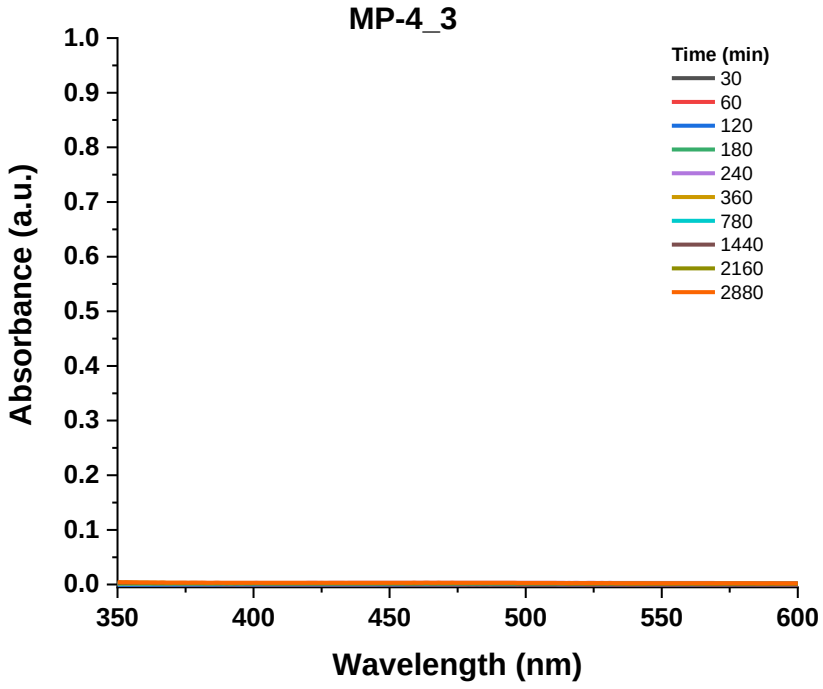

Figure S28: UV/Vis MO Release of MP-4_3

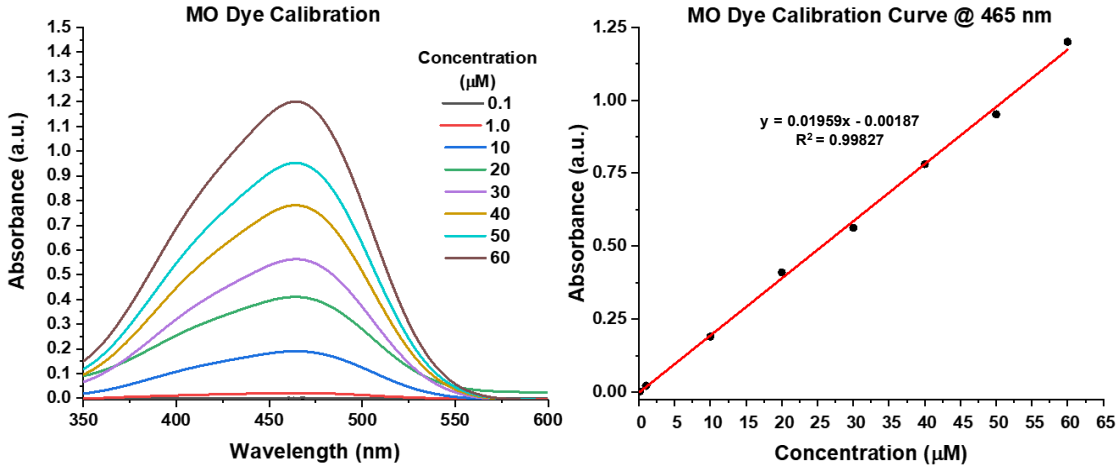

Figure S29: MO calibration curve in MilliQ H_2O.

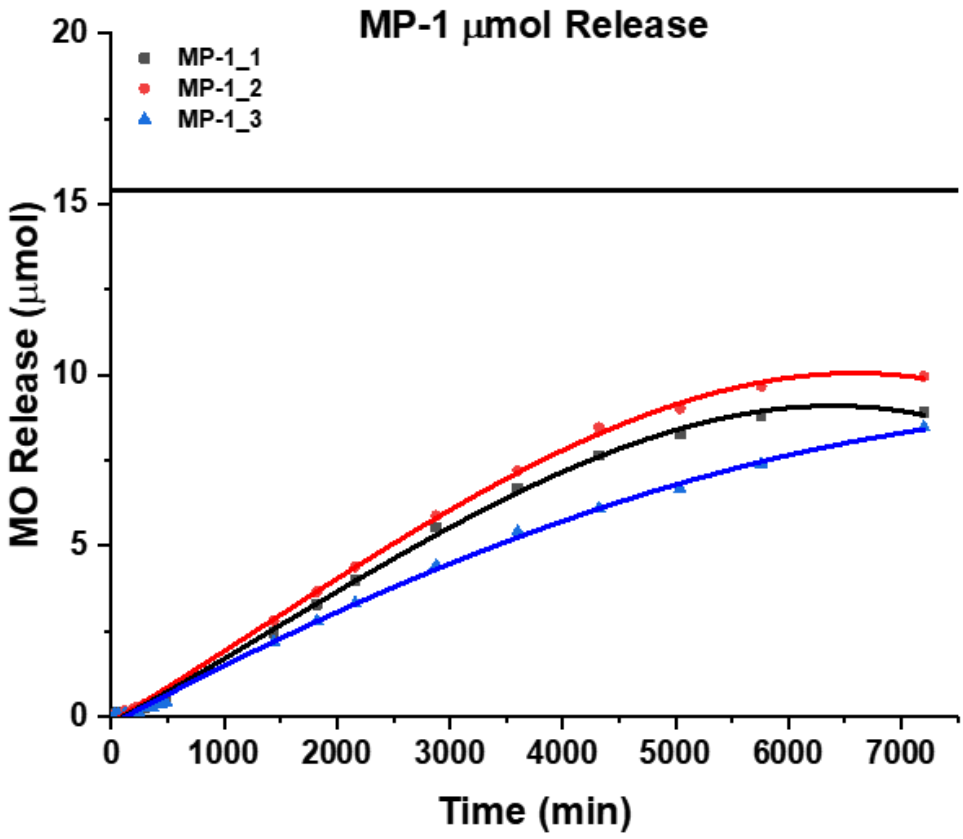

Figure S30: Microparticle sample mol release of MO over time.

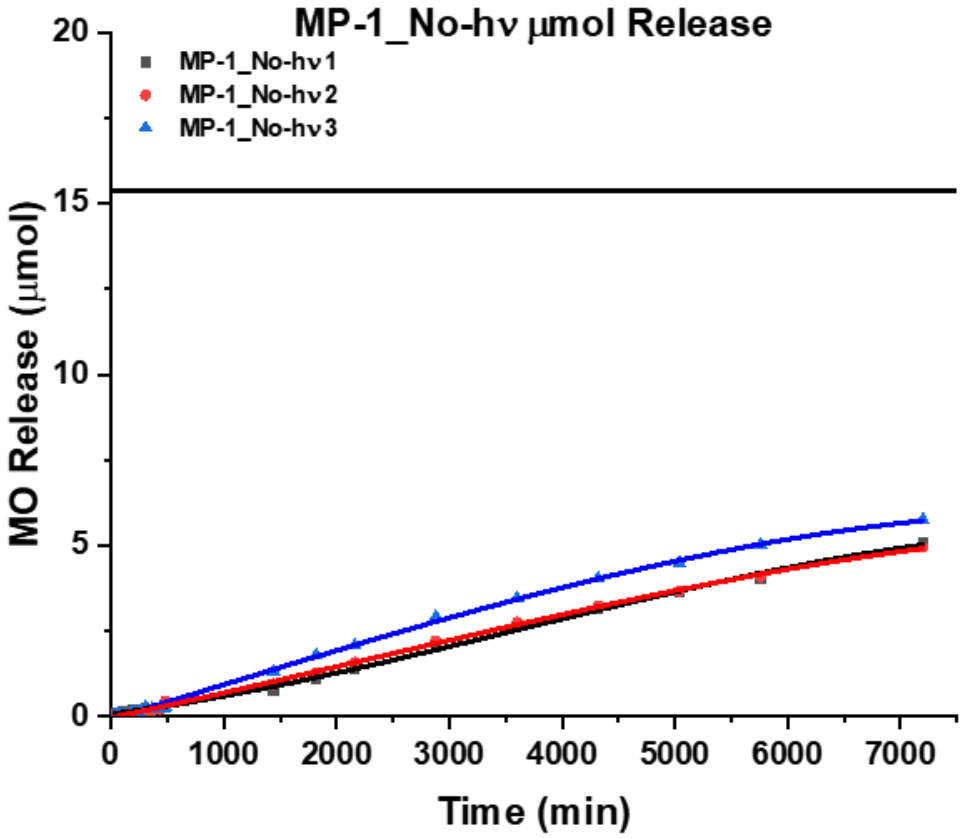

Figure S31: Irradiation control mol release of MO over time.

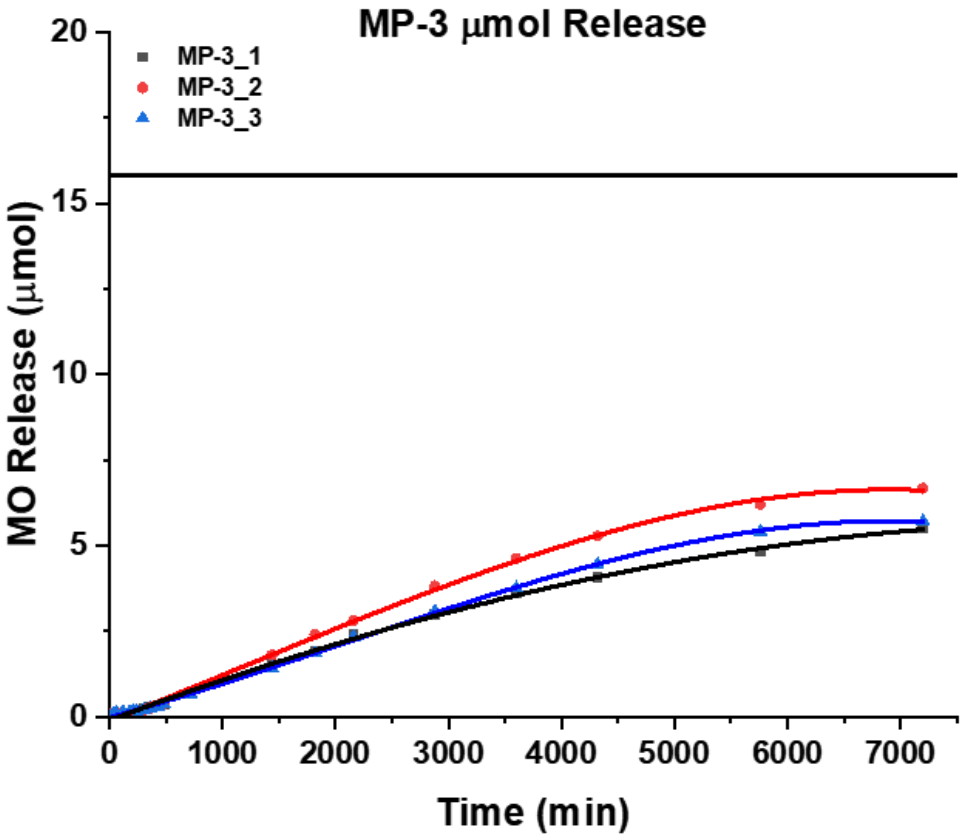

Figure S32: Photocatalyst control mol release of MO over time.

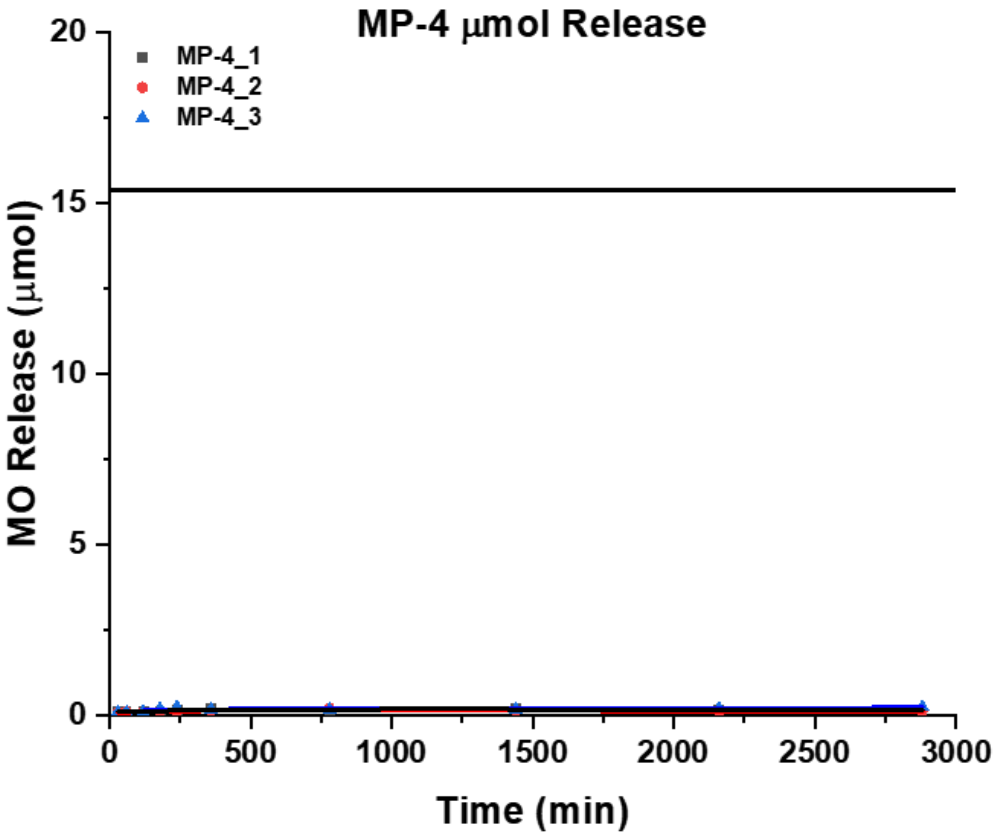

Figure S33: Viologen control mol release of MO over time.

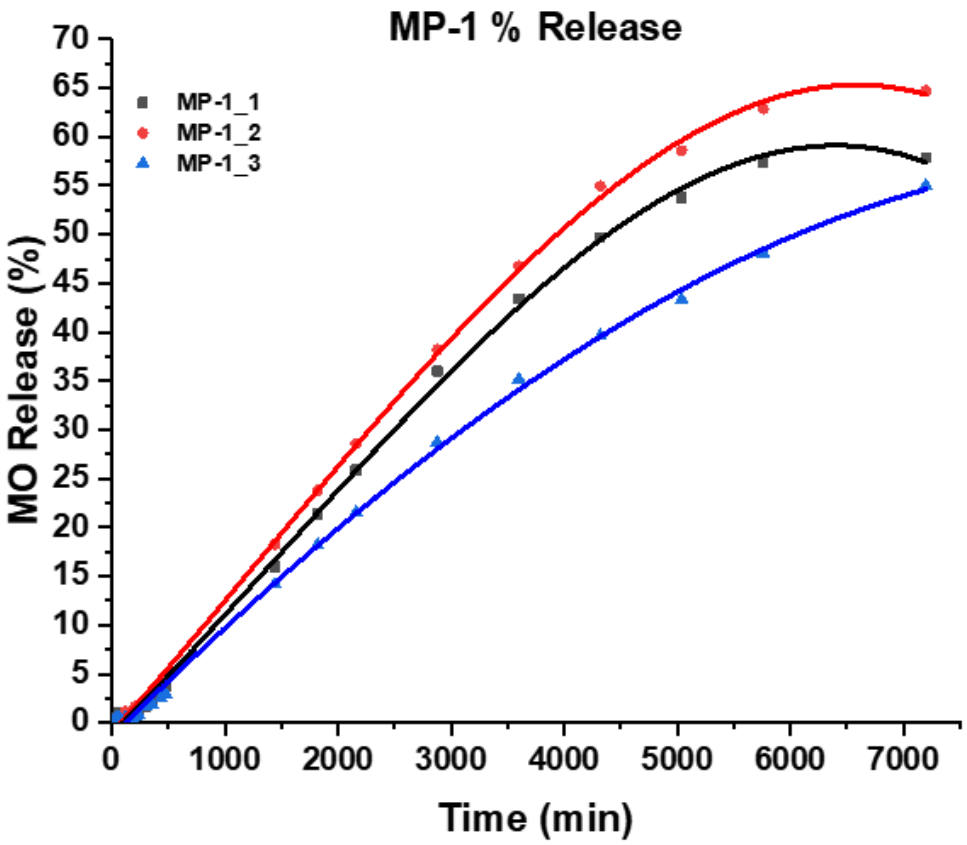

Figure S34: Microparticle sample percent release of MO over time.

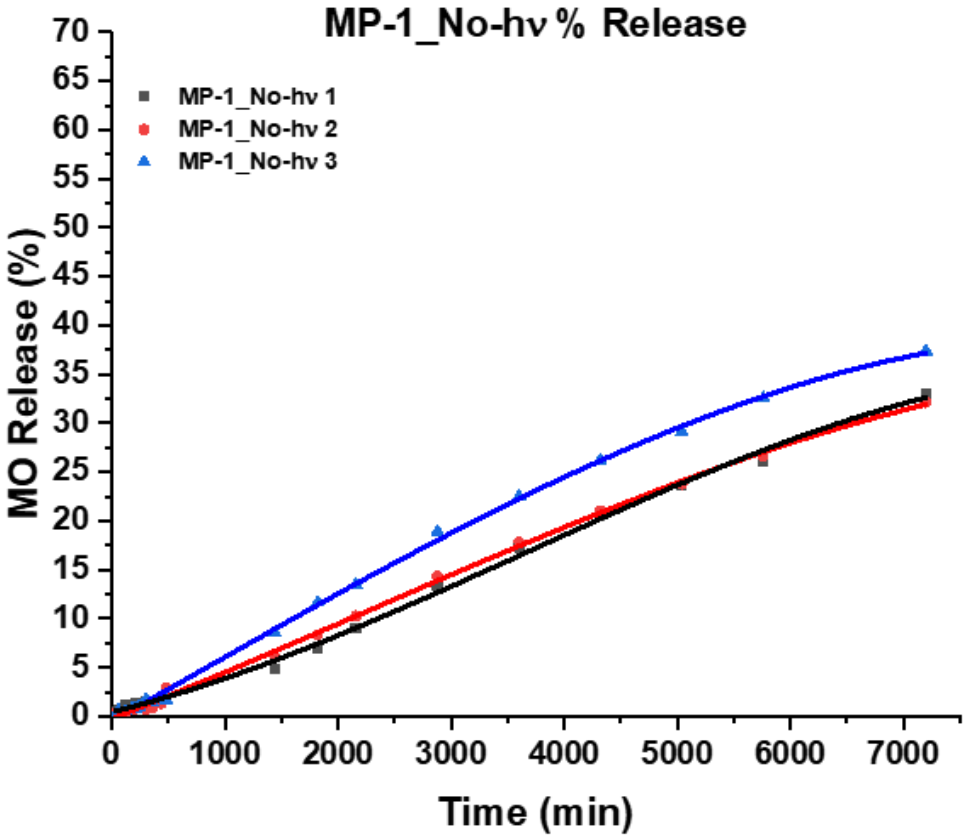

Figure S35: Irradiation control percent release of MO over time.

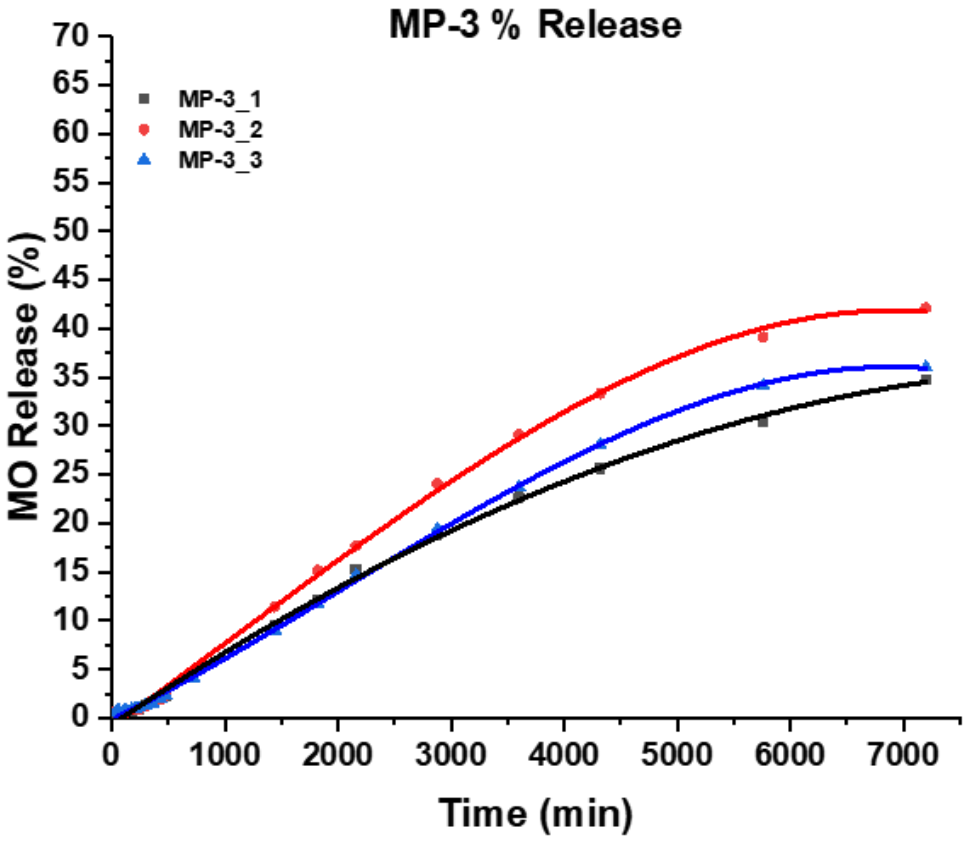

Figure S36: Photocatalyst control percent release of MO over time.

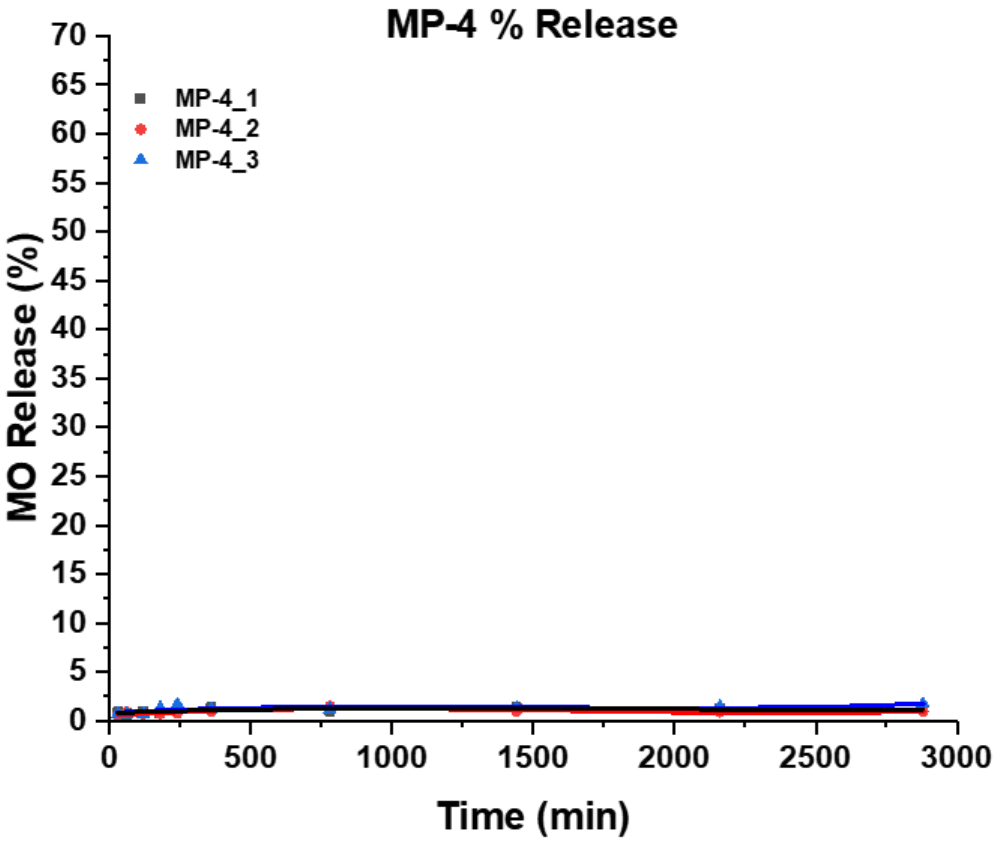

Figure S37: Viologen control percent release of MO over time.

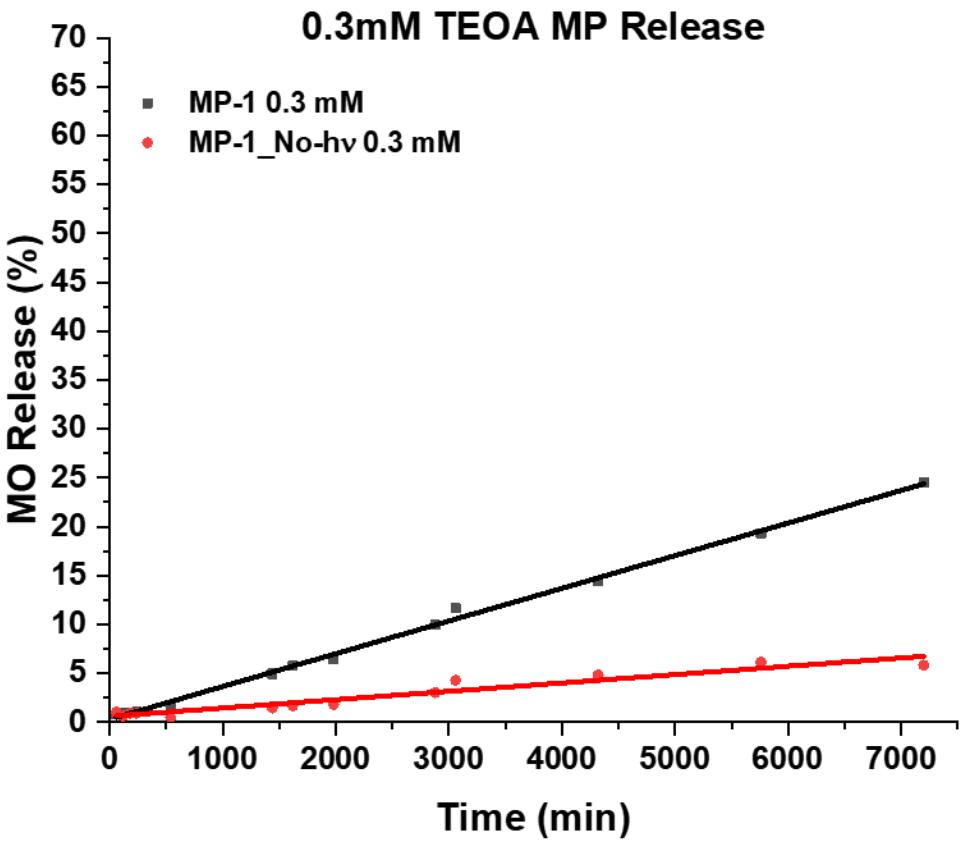

Figure S38: Percent release of MO from microparticles soaked in 0.3 mM TEOA.

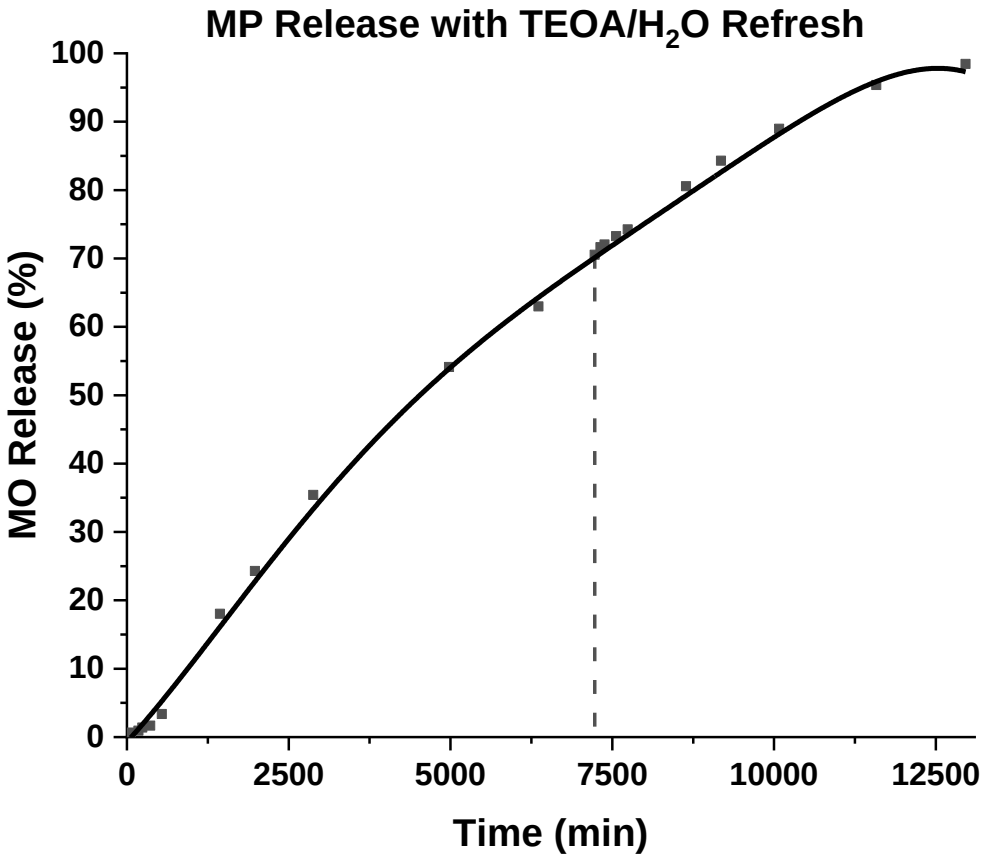

Figure S39: Percent release of MO from microparticles soaked in 3 mM TEOA with an exchange of fresh TEOA/H_2O at 5 d (indicated by dashed line).

Section F. References

1. C. E. McCusker, J. K. McCusker, *Inorg. Chem.* 2011, **50**, 1656–1669.

2. Q. Zhang, J. Dong, Q. Meng, G. Huang, S. Li, *Russ. J. of Gen. Chem.* 2018, **88**, 2388-2393.

3. N. Armaroli, G. Accorsi, D. Felder, J. Nierengarten, *Chem. Eur. J.* 2002, **8**, 2314-2323.

4. X. Schultze, J. Serin, A. Adronov, J. M. Fréchet, J. *Chem. Commun.* 2001, **1**, 1160–1161.

5. F. Amir, X. Li, M. C. Gruschka, N. D. Colley, L. Li, R. Li, H. R. Linder, S. A. Sell, J. C. Barnes, *Chem. Sci.* 2020, **11**, 10910-10920.

6. T. Katagiri, S. Ikeyama, Y. Amao, *J. Photochem. Photobiol. A.* 2018, **358**, 368-373.

7. A. F. Greene, M. K. Danielson, A. O. Delawder, K. P. Liles, X. Li, A. Natraj, A. Wellen, J. C. Barnes, *Chem. Mater.* 2017, **29**, 9498-9508.